

ANL-7071

J. Monaweck, D208

ANL-7071

J. H. MONAWECK

0557

JUL 30 1965

ASSISTANT DIRECTOR  
REACTOR ENGINEERING

# Argonne National Laboratory

REACTOR DEVELOPMENT PROGRAM

PROGRESS REPORT

June 1965

## LEGAL NOTICE

This report was prepared as an account of Government sponsored work. Neither the United States, nor the Commission, nor any person acting on behalf of the Commission:

A. Makes any warranty or representation, expressed or implied, with respect to the accuracy, completeness, or usefulness of the information contained in this report, or that the use of any information, apparatus, method, or process disclosed in this report may not infringe privately owned rights; or

B. Assumes any liabilities with respect to the use of, or for damages resulting from the use of any information, apparatus, method, or process disclosed in this report.

As used in the above, "person acting on behalf of the Commission" includes any employee or contractor of the Commission, or employee of such contractor, to the extent that such employee or contractor of the Commission, or employee of such contractor prepares, disseminates, or provides access to, any information pursuant to his employment or contract with the Commission, or his employment with such contractor.

0557

ARGONNE NATIONAL LABORATORY  
9700 South Cass Avenue  
Argonne, Illinois 60440

REACTOR DEVELOPMENT PROGRAM  
PROGRESS REPORT

June 1965

Albert V. Crewe, Laboratory Director  
Stephen Lawroski, Associate Laboratory Director

<u>Division</u>	<u>Director</u>
Chemical Engineering	R. C. Vogel
Idaho	M. Novick
Metallurgy	F. G. Foote
Reactor Engineering	L. J. Koch
Reactor Physics	R. Avery
Remote Control	R. C. Goertz

Report Coordinated by  
R. M. Adams and A. Glassner

Issued July 30, 1965

Operated by The University of Chicago  
under  
Contract W-31-109-eng-38  
with the  
U. S. Atomic Energy Commission

## FOREWORD

The Reactor Development Program Progress Report, issued monthly, is intended to be a means of reporting those items of significant technical progress which have occurred in both the specific reactor projects and the general engineering research and development programs. The report is organized in a way which, it is hoped, gives the clearest, most logical overall view of progress. The budget classification is followed only in broad outline, and no attempt is made to report separately on each sub-activity number. Further, since the intent is to report only items of significant progress, not all activities are reported each month. In order to issue this report as soon as possible after the end of the month editorial work must necessarily be limited. Also, since this is an informal progress report, the results and data presented should be understood to be preliminary and subject to change unless otherwise stated.

The issuance of these reports is not intended to constitute publication in any sense of the word. Final results either will be submitted for publication in regular professional journals or will be published in the form of ANL topical reports.

The last six reports issued  
in this series are:

December 1964	ANL-6997
January 1965	ANL-7003
February 1965	ANL-7017
March 1965	ANL-7028
April 1965	ANL-7045
May 1965	ANL-7046

# TABLE OF CONTENTS

	<u>Page</u>
I. LIQUID-METAL-COOLED REACTORS	1
A. EBR-II	1
1. Operations	1
2. Building Containment	1
3. Shutdown Coolers	1
4. Reactor Physics	1
5. Fuel Cycle Facility	2
B. FARET	4
1. General	4
2. Reference Core-I Design	5
3. Shielding Windows	5
4. Cell Penetrations	6
5. Design of Core Support	6
6. Core Instrumentation	9
7. Electrical Connectors	9
8. Fuel Assembly Sodium Flow Test Loop	12
9. Argon Enclosure for Fuel-removal Experiments	12
10. Static Test Vessels	12
11. FARET Criticals	12
C. Fast Reactor Systems and Concepts	17
1. 1000-MWe Metal-fueled Fast Breeder Reactor Study	17
D. General Fast Reactor Physics	18
1. ZPPR	18
2. ZPR-9	18
E. General Fast Reactor Fuel Development	21
1. Jacket Materials	21
2. Condition of EBR-II Core-I Fuel	22
F. General Fast Reactor Fuel Reprocessing Development	23
1. Skull Reclamation Process	23
2. Pyrochemical Processes for HTGR and Other Reactor Fuels	26
3. Decladding Studies for TV-20 Cladding	27

## TABLE OF CONTENTS

	<u>Page</u>
4. Materials Evaluation	28
5. Burnup Analysis--Neutron Activation Analysis by the Use of an Internal Flux Monitor	28
II. GENERAL REACTOR TECHNOLOGY	31
A. Experimental Reactor and Nuclear Physics	31
1. In-core Fast-neutron Spectroscopy	31
B. Theoretical Reactor Physics	33
1. Optimal Control of a Nuclear Reactor	33
C. High-temperature Materials	33
1. Ceramics	33
2. Liquid-Metal Corrosion	36
3. Component Surveillance Loop	37
4. Irradiation Testing	38
D. Other Reactor Fuels and Materials Development	38
1. Nondestructive Testing	38
E. Engineering Development	41
1. Two-phase Flow	41
2. Boiling Liquid-Metal Technology	41
3. General Heat Transfer	43
F. Chemical Separations	44
1. Fluidization and Volatility Processes	44
2. General Chemistry and Chemical Engineering	47
G. Plutonium Recycle Reactors	49
1. EBWR Facility	49
III. ARGONNE SYSTEMS RESEARCH AND DEVELOPMENT	51
A. Argonne Advanced Research Reactor (AARR)	51
1. General	51
2. Critical Experiments	51

## TABLE OF CONTENTS

	<u>Page</u>
3. Heat Transfer	56
4. Hydraulic Tests	57
5. Stress Calculations	58
B. Energy-conversion Systems	58
1. Thermionic Energy Conversion	58
IV. NUCLEAR SAFETY	60
A. Reactor Kinetics	60
1. Fast Reactor Safety	60
2. Pressure-pulse Scaling Laws	60
B. TREAT	61
1. Operations	61
2. Large TREAT Loop	61
3. Integral Sodium Loops	62
4. Physics Analysis of TREAT with an EBR-II Subassembly in Test Hole	63
C. Chemical and Associated Energy-transfer Problems in Reactor Safety	64
1. Studies of Transient Heat Transfer	64
V. PUBLICATIONS	67



## I. LIQUID-METAL-COOLED REACTORS

### A. EBR-II

#### 1. Operations

After the scheduled shutdown period for fuel-surveillance studies after nominally 0.8-a/o burnup, the reactor was started on June 10. On June 13, the reactor power was raised to 45 MWt. Operations continued at 45 MWt until 1% maximum fuel burnup had been achieved on June 25, at which time the reactor was shut down and the plant was put in standby condition preparatory to fuel handling for removal of surveillance subassemblies. Total integrated thermal power as of shutdown is approximately 2502 MWd, of which 489 MWd were accumulated during the June operation.

During the run and at various power levels and flows, measurements of power coefficient and noise were made as part of reactor kinetics studies.

#### 2. Building Containment

The two flexible seals around the secondary sodium lines were successfully tested for leak rate to comply with the requirements for reactor containment. The primary tank temperature was lowered to about 380°F and the secondary sodium drained. The primary tank was then heated for fuel-handling operations. The first flexible seal was tested with the primary-tank bulk sodium at 560°F and the second seal with sodium at 580°F. The primary sodium was then cooled to 380°F for filling of the secondary sodium system, followed by reheating to 700°F (plant standby).

#### 3. Shutdown Coolers

A test to determine the capacity for heat removal of the shutdown coolers was completed at a primary tank temperature of 700°F. The measurement was based on inlet and outlet NaK temperatures and flowrates for each shutdown cooler. The total heat removal of both coolers was 363 kW. A more comprehensive test is scheduled since there is some doubt as to the calibration of the flowmeters on the coolers.

#### 4. Reactor Physics

Power-coefficient measurements were carried out for the following sequential increases in power: 0, 10, 25, 30, 37.5 and 45 MW. No change in the general slope of the power-coefficient curve was detected. Approximately 81.9 lh were required to increase the power of the system (at 700°F bulk sodium temperature) from 0 to 45 MW, giving an average power coefficient value of 1.82 lh/MW. The slight increase from 1.74 lh/MW measured at 0.60 a/o burnup is not considered significant.

Four rod-drop measurements were conducted in the power region from 100 to 500 kW and six at 45 MW. (Recent modifications of the linear amplifier feeding the magnetic tape recorder were apparently successful in reducing the influence of extraneous noise.) The results indicated that the modifications essentially eliminated the presence of 60-cps noise and decreased the effects of random extraneous noise by a factor of about four. The results of measurements conducted at low power, however, still indicated the existence of noise components which are almost certainly intrinsically associated with the system. In future measurements at low power such effects will be "averaged out" by carrying out multiple measurements.

All flux recordings taken above 25 MW indicated the existence of a small, 10-cps oscillation. Calculations of the natural vibration frequency of a single fuel assembly in sodium gave 5.1 cps which, in principle, could account for the 10.2-cps oscillation; however, a reactivity perturbation of about 1 lh is needed to account for the amplitude of the signal. All calculations of the reactivity associated with credible amounts of subassembly "flutter" result in values much too small to explain the oscillation amplitude.

## 5. Fuel Cycle Facility

a. Waste Disposal. The use of the EBR-II burial ground for waste has been initiated with the disposal of two cans of waste. One can contained an estimated 1500 curies and showed a radiation level of 80 R at 1 ft; the other contained an estimated 6500 curies and read 250 R at 1 ft.

### b. Irradiated Fuel Processing.

(i) Sodium Removal, Dismantling, and Decanning. Two core assemblies (of 0.75 and 0.56% maximum burnup), one inner blanket, two outer blanket, and one special irradiation subassembly (from General Electric Company) have been cleansed of sodium and dismantled. The GE special irradiation subassembly was transferred to TAN after dismantling, for examination and shipping.

Approximately 300 irradiated fuel pins have been decanned with no problems. The spacer wires continue to remain coiled around the cans on the majority of the elements after shearing.

(ii) Melt Refining and Oxidation. Two melt refining runs with 0.56-0.75% burnup fuel and one irradiated-scrap-consolidation run were made with yields of 92-94%. An increased tendency for the sodium-coated fuel pins to agglomerate and stick in the furnace charger has been noted with increased levels of burnup.

The glowing area in the crucible was again present after the melt refining and slag oxidation runs for this irradiated fuel (see Progress Report for May 1965, ANL-7046, p. 5).

(iii) Fuel Fabrication. Three injection-casting runs were made using irradiated fuel. Approximately 2/3 of the pins cast were acceptable. The major causes of rejection were unsatisfactory diameter (48% of rejects) and porosity (30% of rejects).

An investigation aimed at gaining a better understanding of the eddy-current, fuel pin porosity testing system of the pin processor has been initiated.

The development of a process for separating fuel from miscellaneous scrap generated at the pin-processing station is continuing.

The bond-testing equipment has been removed from the cell because of malfunction.

c. Fuel Surveillance. The examination of the fuel up to 0.75% burn-up indicates no measurable change in can or fuel diameter and very small increases in gas pressure (increase of 0-0.2 atm) in the fuel can. The increase of sodium level in the can for the fuel at 0.75% burnup was 0.42 in.

During the month, two core, one inner blanket, and two outer blanket subassemblies were transferred from the basket to the FCF for cleaning, disassembly, and inspection in accordance with the EBR-II fuel and blanket surveillance program. The following subassemblies were loaded into the storage basket: one reprocessed, core-type, inner blanket; two virgin core and one virgin safety rod; one virgin control rod, and one alpha measurement core-type subassembly.

d. Fuel-handling Modifications and Maintenance. Three heaters failed in the blade of the large rotating plug during seal melting carried out in a program for measurements of changes in the bulk sodium temperature. Grounding of the heater flexible shield to the lead wires caused melting of the flexible conduit connected to the top end of the heater sheath.

The flexible conduit and lead wires were removed from the off-set heater holes. However, the 3-in. long heaters remained stuck in position. Since access to the heaters is quite limited, an extension tool is being designed and built to remove the stuck heaters.

As a temporary expedient, new heaters were installed just above the failed heaters. Their performance in heating the seal alloy is being investigated.

Electrical modifications have been made to Sequence A of fuel handling to permit opening the control-rod gripper jaws at the "down" position of the control-rod lifting platform rather than at the "operate" elevation. This allows the control subassemblies to be released from the gripper jaws without subjecting the latter to the weight of the subassemblies.

The Fuel Unloading Machine (FUM) has been operated for some time without cleaning. As a result, the gripper is hanging up in the transfer port tube, there is an inadequate sense indication of the "loaded" or "unloaded" conditions of the jaws, and excessive sodium has built up in the FUM port drip pan. The transfer port tube was rodded out and the FUM port cleaned. In addition, the scheduled replacement of the FUM gripper was accomplished. The prototype gripper, although still operable, was replaced with an improved Mark II gripper, which has operated satisfactorily.

## B. FARET

### 1. General

The FARET architect-engineering (AE) portion of the Title II Design is approximately 99% complete. All design drawings and specifications for the Title II effort have either been signed by ANL and the Commission or are at the AE's offices ready for signature. The remaining AE work consists of completion of the Title II cost estimate and of some minor design details. This work is scheduled for completion by the end of July.

The drawings and specifications that comprise Design Packages V (Instrumentation and Control) and IX (General Facility) were ready for signature on June 3, 1965. These constituted all the remaining Title II design work. On that date the Commission advised the architect that the signing of these documents was being withheld for an indefinite period until certain matters within the Commission are resolved. Resolution of these matters is still pending.

The AE is rapidly reducing forces as a consequence of pending completion of Title II. The remaining work consists chiefly of (1) completion of the Title II cost estimate, (2) minor corrections to the drawings and specifications and (3) minor design changes requested by the Laboratory. The latter are a number of late items that were withheld during the final few weeks to facilitate an orderly completion of the work.

The start of construction, initially planned for October 1964, is not yet authorized. Neither has the construction manager been authorized to initiate the procurement of Packages III (Liquid-Metal Heat Exchangers) and IV (Liquid-Metal Pumps). These are particularly long-lead items but now that Package II, the reactor vessel, procurement has been initiated, Packages III and IV could soon become the dominating factors in establishing the construction schedule.

An interim report on the project was prepared at the request of the Division of Reactor Development and Technology. The report describes the operating and experimental capability of the facility, the preliminary design of Core I and the design features of the plant. The plant description is based upon the final Title II design--thereby providing a firm description of the FARET facility.

A formal quality assurance procedure for the project is being prepared. This work is in the very early stage of preparation.

## 2. Reference Core-I Design

Work continues on the detailed design of Core I, in which will be tested fuel elements similar to those expected to be used in the 200-300-MW(e) Prototype Reactor of the AEC's Fast Reactor Development Program (see Progress Report for February 1965, ANL-7017, p. 15). It is planned that the Core-I loading will include mixed-oxide, -carbide, and -metal fuels, operating under forecast prototype reactor conditions. Each type of fuel will be installed in several different forms in order to test the effects of various significant parameters. For example, both vibratory-compacted, together with pressed and sintered ceramic, fuels are being considered. Cladding materials such as 304 H stainless steel and Incoloy-800 for the ceramic fuels are being seriously considered. Cladding wall thickness will vary, to weigh the effects of decreasing pressure stresses at the expense of increasing thermal stresses. Differing heat flux exposure will be imposed.

The present schedule requires that the reference design details of Core I will be completed by Sept. 1, 1965. Procurement of a dummy Core-I subassembly, similar to the instrumented subassembly illustrated in the May report (see Progress Report for May 1965, ANL-7046, p. 8) is almost complete.

## 3. Shielding Windows

The reference design for the cell shielding windows (see Progress Report for Oct 1964, ANL-6965, p. 58) incorporated successfully proven concepts used in the 31 shielding windows purchased by the Laboratory for the EBR-II Fuel Cycle Facility as follows:

1. Low cerium content in the lead glass for the slabs receiving most intensive radiation (all glass for oil laminated tank unit);
2. The specification of a hydrochloric acid leach treatment for the three dry-framed slabs A-2, B-1, and B-2. When such an acid bath treatment is set up with proper normality of the solution, and control of temperature and time of immersion, a uniform surface etching is produced which reduces the normal reflectivity of air-glass interfaces from 5% per surface to 2.5%.
3. Primary gastight sealing of the window to contain the argon gas cell atmosphere was to be accomplished by gasketing slab B-2 directly to a machined surface of the liner. In the case of the Fuel Cycle Facility window, the corresponding seal was made with a 1 in. thick plate of glass. It has been demonstrated in tests that the same sealing technique is reasonable with a glass slab  $8\frac{1}{2}$  in. thick.

4. Removable glass bearing components.

5. A secondary gas seal at the operations face of the window which bridges the peripheral gap between the tank face and the steel window liner allowing for minor misalignment of the tank unit due to normal fabrication tolerances.

Despite this past successful experience, only one bid was received on an alternative design conceived by one manufacturer, and this design is not completely acceptable.

Recently, the specification for the cell wall was changed from 220-lb/cu ft concrete to 147-lb/cu ft concrete. In the reference window design, the removal of glass slabs T-2 and T-3 from the tank unit, and replacement by oil, would give a window matching the new wall in shielding ability and would affect the viewing angles only slightly. This matching cannot be accomplished as readily in the alternative design as proposed in the manufacturer's bid.

The shielding window design and specifications are being reviewed to enable more manufacturers to bid.

#### 4. Cell Penetrations

A mockup of the electrical-service penetration of the FARET cell wall (see Figure 1) has been designed and is now being assembled. This test unit has internal components made to accommodate rubber-covered electrical cables. The internal components may be removed and replaced with components suited for other types of service. The assembled penetration will provide means continuously to test leak tightness, and periodically to test structural strength and ascertain shielding value.

Preliminary leak tests have been conducted with the partially assembled penetration and components. The total leak rate of gases in these tests at 30 psig of air was less than  $0.5 \text{ ft}^3/\text{day}$ . Leakage through the cable has been most difficult to seal and accounts for about  $3/4$  of the experimentally determined leak rate. A method of potting the cable ends has been incorporated. Electrical cables of the actual type and size have been ordered.

#### 5. Design of Core Support

The CDC-3600 computer program for the strength and deformation analysis of the FARET two-plated fuel-support structure is now workable. It treats a structure consisting of two circular plates reinforced by a concentric row of tubes between them. Both plates have the same outside

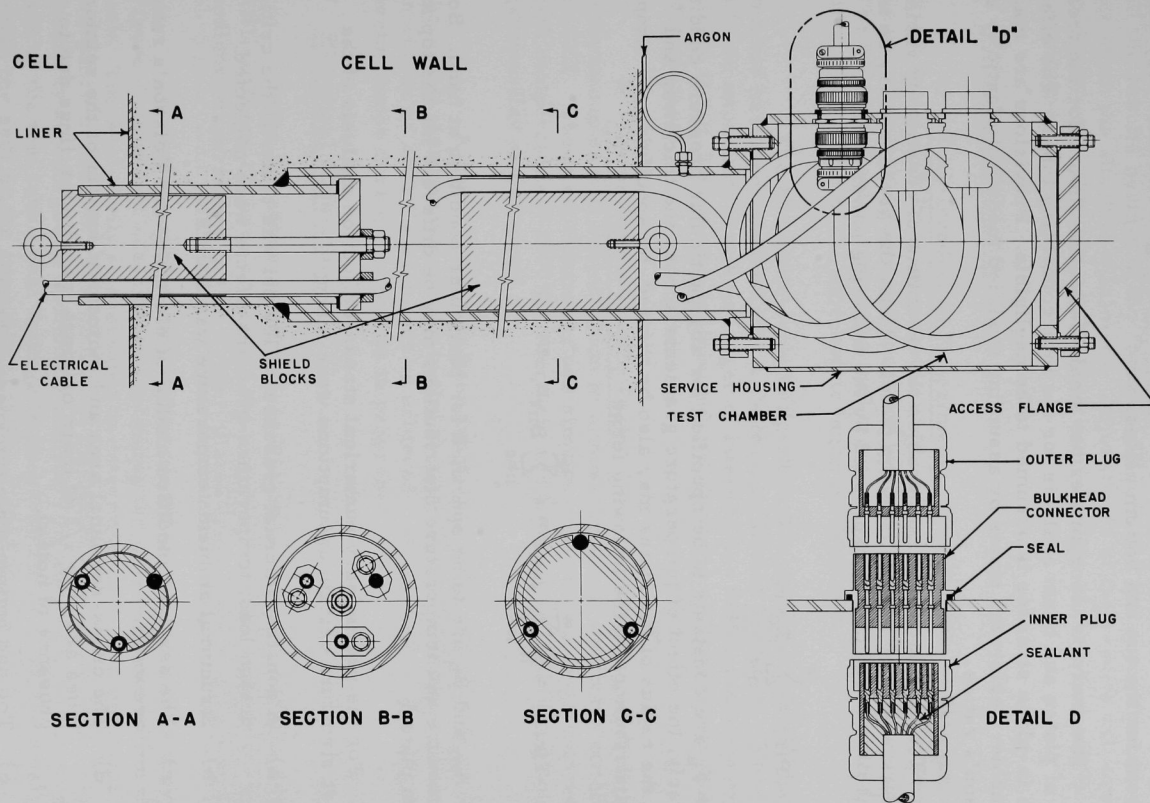


Figure 1. Electrical Service Penetration of FARET Cell Wall

radius but may have different thicknesses and different material properties as long as they are constant for each plate. The edge restraints may be different for the top and bottom plates.

The analysis incorporates the small-deflection theory for the treatment of plates and beam analysis for the interconnecting tubes. The effect of the in-plane stresses is assumed to be negligible. Provisions are made to consider perforated plates by assuming modified moduli of elasticity and Poisson's ratios.

The computer program enables the treatment of constant or variable pressure along the radius ( $r$ ) of the plates. Thus, the pressure may be any distribution which can be expressed by the following power series:

$$P(r) = \sum_{n=0}^{\infty} F_n r^n,$$

where  $F_n$  are constants to be specified for any particular pressure condition. Similarly, the effect of temperature gradients across the thickness and along the radius of the plates may also be treated, by specifying the temperature distributions in the following form:

$$T(r, z) = \frac{z}{h} \sum_{m=0}^{\infty} A_m r^m + \sum_{n=0}^{\infty} B_n r^n,$$

where  $A_m$  and  $B_n$  are to be specified for particular condition at hand. Both the pressure and temperature distributions may be different for the top and bottom plates.

For the preliminary numerical stress-deflection analysis of the support structure certain assumptions were made:

- a) A constant internal pressure of 100 psi was taken as the critical design load; temperature-gradient effects were neglected.
- b) Structural ambient temperature was 1000°F.
- c) The assumed modified moduli of elasticity and Poisson's ratios are valid.
- d) The cross-sectional area and moment of inertia of the reinforcing tubes are only 1/2 of their original magnitudes (loss due to presence of holes).
- e) Top and bottom plate thicknesses are the same.
- f) Both plates have simply supported edges.

In the analysis it is also assumed that the tubes are all located at the same distance from the center--the average radius. Correspondingly, all the results pertain to the "averaged" case and the maximum values do not mean the absolute maximum. Adjustments of the results will need be made but once when a more definite configuration of the structure is established.

## 6. Core Instrumentation

a. Fuel-irradiation Experiments. The analysis of data taken from W-3% Re/W-25% Re thermocouple used in the Plutonium Fuel Irradiation Experiment (see Progress Report for May 1965, ANL-7046, p. 10) continues. The initial indicated centerline fuel temperature of 1150°C increased with time. The cause of the increase is being investigated.

The plutonium-fueled slip-fit fuel capsule inserted in the CP-5 reactor has been replaced with a thermocouple test specimen. Since the slip-fit experiments are no longer of interest, the fuel-irradiation experiments in CP-5 have been terminated and replaced with the thermocouple test program.

b. Thermocouple In-pile Tests. The in-pile testing of fuel-pin thermocouples will subject them to almost the actual operating condition in FARET. These conditions include simultaneous thermocouple exposure to high temperature (>2000°C), thermal- and/or fast-neutron fluxes, and a gamma-flux environment.

A new capsule has been fabricated which can contain up to three test thermocouples. An initial test has indicated that temperatures in excess of 2400°C can in fact be achieved. An analysis of the thermocouple performance during this test is in progress.

## 7. Electrical Connectors

Tests in sodium at 650°C (see Progress Report for March 1965, ANL-7028, p. 12) have confirmed the results of earlier tests at lower sodium temperatures in that copper-plated seals showed most promise.

The test apparatus constructed for these experiments is shown in Figure 2. The test seal fixture containing the seal is placed within the test tank. The seal cavity is evacuated to determine seal tightness prior to submergence in sodium. The vacuum is maintained during the test. The seal fixture is submerged in sodium by transferring sodium from the storage tank to the test tank. Seal leakage is observed either from the level probe within the seal or the condition of the seal after disassembly.

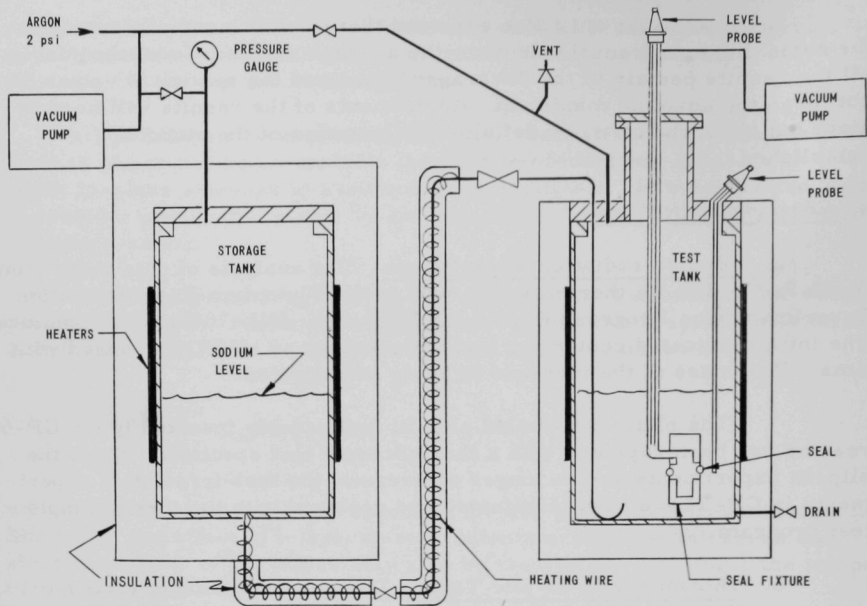


Figure 2. Connector Seal-test Apparatus

Another type of seal incorporates a gasket free seal face and relies on internal pressurization to prevent sodium from entering. A model of this type of seal (Figure 3) has been fabricated and tested first in water and then in sodium. In the water test, a gas out-leakage less than  $0.1 \text{ ft}^3/\text{day}$  was observed at 6 in. W.G. and no water in-leakage. Identical conditions were maintained in the sodium test except for the temperature of  $700^\circ\text{F}$ .

Three test cycles were performed in the connector test assembly, each consisting of submersion in sodium for a ten minute period, then lowering of the sodium level below the connector and complete separation of the two connector halves. No sodium in-leakage was experienced.

Owing to the fact that a positive pressure in the tests tank rather than negative pressure in the dump tank was used to change the sodium level around the electrical connector, the 6 in. water column differential pressure across the sealing surface was not maintained at all times during sodium submersion and resulted in flooding of the contact pin area with sodium. A change in test procedure which will prevent this condition is planned for the next series of tests.

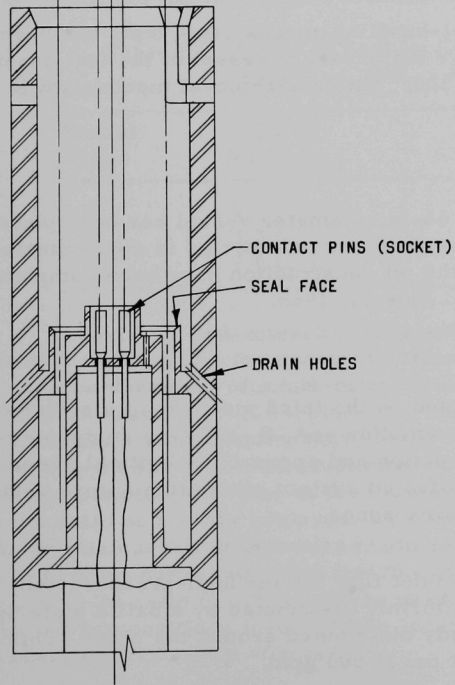
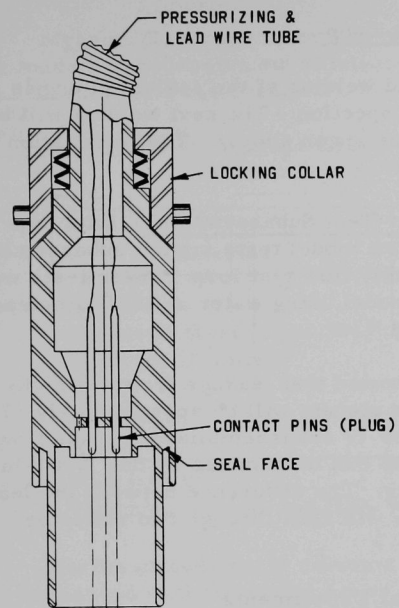


Figure 3  
FARET Electrical Connector  
Gasketless Model

## 8. Fuel Assembly Sodium Flow Test Loop

a. Loop Construction. Field welding of the sodium piping is complete except for final radiographic inspection. The next welding will be done on the 1-in. blanket-gas lines for argon supply. The installation of thermal insulation is continuing.

b. Orifice Determination for Test Subassemblies. Inlet hole sizes have been established by means of flow model tests for the subassemblies to be installed in the 1200°F fuel assembly flow test loop. These tests were conducted on a single subassembly model using water at 100°F, instead of sodium at 860°F, as the working fluid.\*

The results of the test showed that leakage from the high-pressure plenum to the low-pressure plenum will be approximately 57 gpm at a pressure differential of 80 psi for 19 subassemblies. Bypass flow of 47 gpm from the low-pressure plenum can be supplied by one 1.001-in. hole in place of the now existing drain plug. The difference between the leakage and the bypass flow, equal to 10 gpm, will flow through two reflector assemblies.

## 9. Argon Enclosure for Fuel-removal Experiments

The enclosure for the fuel-handling-mechanisms tests has been completed and installed directly above the pressure vessel of the fuel assembly flow test loop vessel in Building 308. The fuel-removal mechanism is being fabricated.

## 10. Static Test Vessels

A purchase order for the 66-in.-diameter vessel has been placed with the Stearns-Rogers Mfg. Co. Delivery is expected in approximately 90 days. The specifications for the pit construction have been completed and issued to potential bidders on June 21, 1965.

## 11. FARET Criticals

Experiments were completed on the third mock-up of a series of cores in ZPR-3 designated as Assemblies 46A, B, and C to study the possible fuel loadings for FARET. Construction and approach to critical are under way on a fourth core, 46D, a multifueled system simulating a core using oxide, carbide, and metal in separate zones.

---

\*In the actual proof test loop, the inlet flow for the high-pressure sub-assembly inlets will be more uniformly distributed by a baffle plate by using forty (40), 1-in. holes evenly distributed around the plate. This should give a pressure drop of 1 psi at 800 gpm.

Measured average worths of materials in Core 46C, relative to void, were made by successive substitutions in 14 drawers distributed in the core. Table I lists the results.

Table I. Average Reactivity Worths of Materials  
in Core C of ZPR-3 Assembly 46

Material	Reactivity Coefficient (Ih/kg)
Sodium	55
Stainless Steel (Type 304)	10
Depleted Uranium <sup>a</sup>	7
U <sub>3</sub> O <sub>8</sub> <sup>a</sup>	17
Carbon	116
Oxygen <sup>b</sup>	74

<sup>a</sup>0.2 w/o U<sup>235</sup>

<sup>b</sup>Derived from U and U<sub>3</sub>O<sub>8</sub> worths

Worths of sodium, in columns running the axial length of the core, were measured in three radial zones in Core 46C. Table II gives the radii of the zones and the Na worths, relative to void, in the zone.

Table II. Worths of Sodium Columns vs. Radius in  
Core 46C of ZPR-3 Assembly 46

Radial Zone	Zone Radii (in.)	Reactivity Coefficient for Axial Columns (Ih/kg)
I	0 to 1.4	51
II	3.3 to 5.1	53
III	7.6 to 9.9	55

A series of fuel-interchange experiments was carried out with Core 46C to ascertain the reactivity effects which would occur in FARET from the replacement of oxide-core subassemblies by carbide- or metal-fueled subassemblies. A carbide-core drawer was constructed, representing a FARET core subassembly with 36 v/o fuel (PuC-UC), 38 v/o sodium, and 18 v/o steel. This was substituted for oxide-core in three radial locations and also for reflector at the core edge. In this carbide simulation, a U-Pu ratio of 6:1 was achieved, with the uranium enrichment averaging 49%. Similar substitutions were made with a core drawer simulating a Pu-U-Ti alloy metal fuel, with the 30 a/o Ti in the alloy represented by steel, a U-Pu ratio of 3.7:1, and the uranium enriched to 14%. Table III gives the compositions involved, the locations of the fuel interchanges, and the resulting reactivity effects.

Table III. Fuel-interchange Experiments in Core C of  
ZPR-3 Assembly 46

1. Compositions of Core Types and Reflector

Drawer Loading	Composition, $10^{22}$ atoms/cc							
	Pu <sup>a</sup>	U <sup>235</sup>	U <sup>238</sup>	Na	Steel <sup>b</sup>	O	C	Al
Oxide Core	0.112	0.334	0.348	0.843	1.539	0.866	0.502	-
Carbide Core	0.170	0.448	0.447	0.843	1.481	-	0.111	-
Alloy Core	0.276	0.129	0.840	0.843	2.230	-	-	-
Reflector	-	-	-	0.211	6.380	-	-	0.305

<sup>a</sup>Isotopic composition: 95.0 a/o Pu<sup>239</sup>, 4.5 a/o Pu<sup>240</sup>, and 0.4 a/o Pu<sup>241</sup>.

<sup>b</sup>Type 304 stainless steel.

2. Replacement Experiments

Drawer Location <sup>a</sup>	Substitution (in 0.78-liter section)	Reactivity Change (Ih)
1-P-17	Carbide for oxide	+129
1-R-17	Carbide for oxide	+102
1-T-17	Carbide for oxide	+55
1-U-17	Carbide for reflector	+127
1-S-20	Carbide for reflector	+174
1-P-17	Alloy for oxide	+42
1-R-17	Alloy for oxide	+30
1-T-17	Alloy for oxide	+11
1-U-17	Alloy for reflector	+92
1-U-17	Oxide for reflector	+90

<sup>a</sup>Refer to Progress Report for May 1965, ANL-7046, p. 13,  
Figure 4.

Radial and axial traverses with both fission counters and reactivity samples were run through the 46C assembly. The counters traversed included fission detectors of U<sup>235</sup>, U<sup>238</sup>, and Pu<sup>239</sup>, and also a B<sup>10</sup>F<sub>3</sub> proportional counter. The results from the axial traverses of the Pu<sup>239</sup>, U<sup>238</sup>, and B<sup>10</sup>F<sub>3</sub> counters are shown in Figure 4 and the results in the radial direction are shown in Figure 5. The reactivity samples traversed were small cylinders of plutonium, enriched uranium, natural uranium, and B<sup>10</sup>; the data from these experiments are being processed.

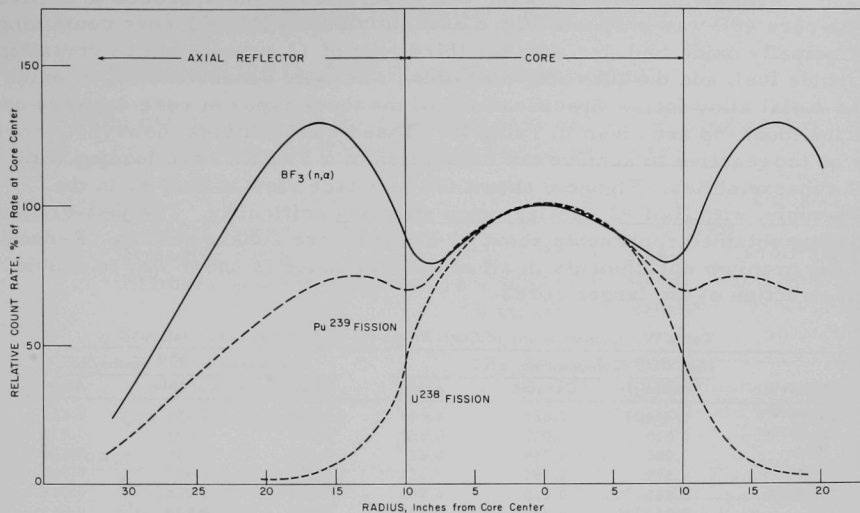


Figure 4. Axial Traverses of Neutron Detectors through ZPR-3 Assembly 46C

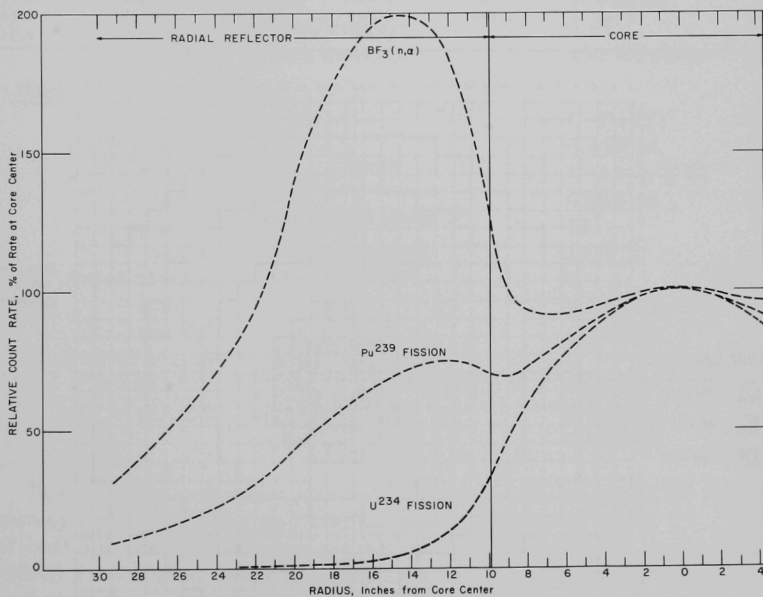


Figure 5. Radial Traverses of Neutron Detectors through ZPR-3 Assembly 46C

With the completion of the 46C experiments, the approach to criticality with core 46D was initiated. Core 46D simulates a FARET core containing principally oxide fuel, but with the third ring of 12 subassemblies containing carbide fuel, and the fifth ring containing alternate subassemblies of oxide and metal alloy fuels. Specifications of the three types of core drawers used in the mock-up are given in Table IV. These compositions, however, proved to be too reactive to achieve the simulation of a FARET core loading with 61 subassemblies. Figure 6 shows the interface view of Half #1 in the assembly, with Half #2 similar, upon attaining criticality. The just-critical loading obtained represents about 51 FARET core subassemblies. Reduction of the uranium enrichments in all of the fuel zones is under way to enable construction of the larger cores.

Table IV. Compositions of Core Zones for ZPR-3 Assembly 46D

Material	Composition, g/cc			Composition, $10^{22}$ atoms/cc		
	Oxide	Carbide	Alloy	Oxide	Carbide	Alloy
Pu <sup>239+241</sup>	0.424	0.621	1.045	0.107	0.156	0.263
Pu <sup>240+242</sup>	0.020	0.030	0.050	0.005	0.008	0.013
U <sup>235</sup>	1.085	1.748	0.437	0.278	0.448	0.120
U <sup>238</sup>	1.579	1.765	3.351	0.399	0.447	0.848
U <sup>234+236</sup>	0.015	0.025	0.006	0.004	0.006	0.015
Na	0.321	0.321	0.321	0.843	0.843	0.843
O	0.230	-	-	0.866	-	-
C	0.100	0.220	-	0.502	1.111	-
Fe	1.019	0.981	1.058	1.099	1.057	1.141
Cr	0.255	0.246	0.265	0.295	0.284	0.307
Ni	0.141	0.136	0.147	0.145	0.140	0.144
Zr	-	-	0.480	-	-	0.317

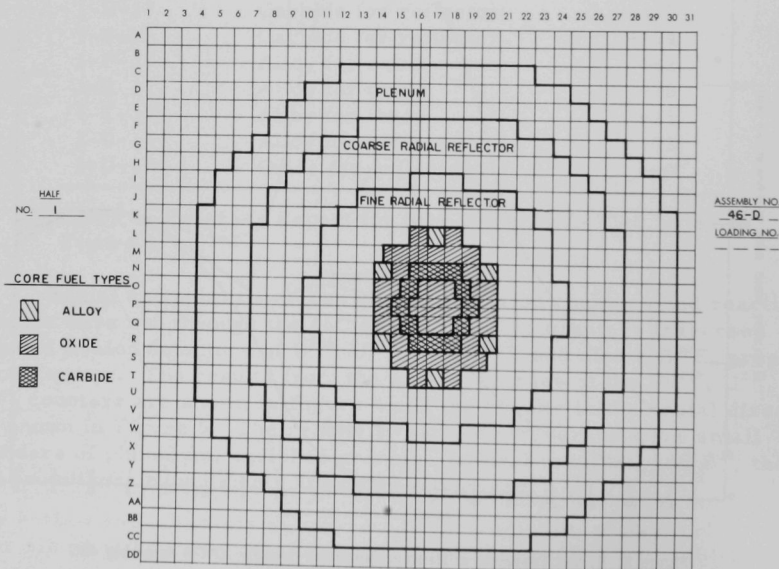


Figure 6. Interface View of ZPR-3 Assembly 46D

## C. Fast Reactor Systems and Concepts

### 1. 1000 MWe Metal-fueled Fast Breeder Reactor Study

The calculations for the reference fast reactor study have been completed. The basic data for the reference design as follows:

#### General

Reactor power	2513 MWt
Breeding ratio	1.48
Primary sodium temperature - inlet	720°F
- outlet	1000°F
Steam	
Pressure	1800 psi
Temperature	900°F
Net plant efficiency	39.8%

#### Reactor

Number of modules	6
Core height	91 cm
- equivalent diameter/module	105 cm
- volume/module	785 liters
- power/module	360 MWt
- power fraction/module	0.85
- average power density	450 kW/liter

#### Fuel

- fuel alloy	U-Pu-Ti
Core pin, OD	0.210 in.
- clad	V-20 w/o Ti
- clad thickness	0.018 in.
- pins/subassembly	331
- maximum $\phi$ temperature	1439°F
Axial blanket - fuel	U
- clad	V-20 w/o Ti
- pin OD	0.210 in.
Radial blanket - fuel	U
- clad	V-20 w/o Ti
- pin OD - inner	0.210 in.
- outer	0.580 in.

The fuel cycle facility studied has a capacity of about 90 metric tons per year of combined core and blanket fuels in ratio of about 1:2. The total capital cost for the facility was established at \$20,800,000, on the basis of the EBR-II Fuel Cycle Facility costs as a basis for cost development. This cost includes processing, fabrication, and waste storage. The wastes are held on site until the heat generation can be dissipated readily by air cooling. The annual operating cost is about \$11,000,000.

## D. General Fast Reactor Physics

### 1. ZPPR

The specifications and drawings for Title II from the architect-engineer have been reviewed and returned with corrections and comments.

The status of items already negotiated or in process of negotiation follows:

a. Reactor Bed and Tables. The contract was signed by the supplier, Giddings and Lewis Machine Co., Fond du Lac, Wisconsin. The delivery date for these items is June 1, 1966. A preliminary meeting with Giddings and Lewis personnel and ANL personnel was held to develop mutually acceptable inspection and quality-control procedures for these specific items.

b. Matrix Drawers. The purchase order for the ZPPR matrix drawers was placed with Mechanical Products Manufacturing Company, Seattle, Washington on June 21. This order is to be completed within 32 weeks.

c. Matrix Tubes. Review of the bids for the matrix tubes is in progress.

d. Poison Safety Rod Drives. The drawings and specifications have been completed, and the bid package sent out.

e. Nuclear Instrumentation. Specifications have been completed and are being reviewed.

f. Other ANL-furnished Items. Work is continuing on reactor knees, source drive, control-rod-position indicators, and the poison-filled safety blades and sheaths.

Construction of the outside electrical- and steam-systems package has been started. This package is scheduled to be completed in August 1965.

### 2. ZPR-9

The boron ring experiment previously performed on Assembly No. 6 was repeated with Assembly No. 6A to determine the effect of adding hydrogen to the reflector on the reactivity controlled boron ring. As the various sectors of the ring were added, the core dimensions were kept constant in order to maintain a constant radial leakage. Compensation for loss of reactivity was made by adding fuel to the central region of the core. Results are shown in Table V.

Table V. Boron Ring Experiment with Assembly 6A of ZPR-9

Run	Boron		Reactivity, 1h		
	Column to Which Added	Accumulated Weight (g)	Excess	Difference	Accumulated
6A-1	Reference		191.963	-	-
2	6	121.8 ± 3.3	142.504	-49.459	-49.46
3	8	284.2 ± 7.7	81.050	-61.454	-110.913
4	8	446.6 ± 12.1	22.509	-58.541	-169.45
5	Fuel Added		206.455	+183.946	-
6	8	609.0 ± 16.5	145.174	-61.281	-230.74
7	8	771.4 ± 20.9	98.742	-46.432	-277.167
8	12	1015.0 ± 27.5	23.549	-75.193	-352.360
9	Fuel Added		210.469	+186.920	-
10	8	1177.4 ± 31.9	149.382	-61.087	-413.447
11	8	1339.8 ± 36.3	109.951	-39.431	-452.878
12	8	1502.2 ± 40.7	67.776	-42.175	-495.053
13	8	1664.6 ± 45.1	34.753	-33.023	-528.076
14	6	1786.4 ± 48.4	5.012	-29.741	-557.817

A single column of boron consists of five cans forming a slab 10 in. long, 2 in. wide, and 1/8 in. thick, and has a total  $B^{10}$  content of  $20.3 \pm 0.55$  g. The quoted error includes the rms dispersion in empty can weights, boron enrichments, nonboron content, and packing density within the cans. With a complete loading (440 cans), 1.786 kg of  $B^{10}$  controlled 1.30%  $\Delta k/k$  over a total subtended angle of  $268^\circ$ . The same loading and distribution of  $B^{10}$  in Assembly No. 6, which had no hydrogen in the reflector, controlled 0.67%  $\Delta k/k$ .

To estimate the effect of extending the 10-in. long boron columns to the actual core length (12 in.), an extra  $2 \times 2 \times 1/8$ -in. can was added to 26 of the 88 boron columns in Assembly No. 6. This removed 17.70 1h reactivity. Extrapolation for a complete boron ring yielded 1.43%  $\Delta k/k$  as the reactivity controlled by the  $B^{10}$ . The corresponding number for Assembly No. 6 was 1.01%  $\Delta k/k$ .

Assembly No. 7 will be constructed next with a core that will have the same composition as in Assembly No. 6 and 6A, but the reflector material will be  $Al_2O_3$  rather than aluminum. Preliminary estimates of the worth of  $Al_2O_3$  relative to aluminum were determined by selectively replacing reflector material of Assembly No. 6A with  $Al_2O_3$  (see Table VI). As was done with the boron ring experiment, fuel was removed from the center of the core in order to maintain a constant radial leakage throughout the experiment.

Loading No. 37 represents a 5-cm ring of  $Al_2O_3$  between the core and the radial, hydrogenated aluminum reflector at a mean radial distance of 37.5 cm. Assuming an exponential loss of worth with radial distance with a relaxation length of 11.6 cm (based on reflector studies with Assembly No. 5), the next 5-cm-thick ring (at 42.5 cm) is expected to have a worth

of 2.8%  $\Delta k/k$ . Extending this procedure through the 30-cm-thick reflector led to a prediction of the worths listed in Table VII.

Table VI. Studies of  $\text{Al}_2\text{O}_3$ -reflector Worth

Run	$\text{Al}_2\text{O}_3$ Reflector		Reactivity, $\text{Ih}$
	Drawers Replaced	Accumulated Weight (kg)	$\frac{\text{Accumulated Worth}}{\text{Accumulated Weight}}$
6A-17	Reference		
18	8	46.419	1.76
19	8	92.838	1.89
20	Fuel Removed		
21	8	130.259	1.98
22	8	184.730	1.83
23	Fuel Removed		
24	8	230.326	2.66
25	8	277.129	2.55
26	Fuel Removed		
27	8	322.725	2.54
28	Fuel Removed		
29	8	369.144	2.65
30	Fuel Removed		
31	8	415.563	2.61
32	8	461.982	2.58
33	Fuel Removed		
34	8	508.401	2.56
35	Fuel Removed		
36	8	554.820	2.55
37	3	572.227	2.52

Table VII. Predicted Worth of  $\text{Al}_2\text{O}_3$ -reflected Material Relative to Aluminum Metal

Position of 5-cm Ring	Worth	
	of Ring	Accumulated
37.5	3.35	3.35
42.5	2.08	5.43
47.5	1.42	6.85
52.5	0.92	7.77
57.5	0.59	8.36
62.5	0.39	8.75
67.5	0.25	9.00

## E. General Fast Reactor Fuel Development

### 1. Jacket Materials

a. Vanadium Alloys. Vanadium-titanium-base alloys have generally favorable combinations of properties for use as jacketing materials for various potential fast-reactor fuels, including the uranium-plutonium-fission fuel alloys. Vanadium-20 w/o titanium (TV-20) is one of the outstanding vanadium-titanium alloys for uses of this type. Some properties, particularly the high-temperature properties, have not been fully investigated. Tests are under way to determine these properties and to ascertain how they may be improved by various modifications of composition. Screening tests of fabricability and of various properties, including resistance to corrosion in oxygen-bearing sodium and compatibility with some fuel alloys, indicate that chromium-bearing modifications of vanadium-titanium bases are among the more promising.

(i) Mechanical Properties. Strain-time curves for V-Ti and V-Ti-Cr alloys are shown in Figure 7 as determined from tensile creep tests in a vacuum (down to  $10^{-6}$  mm Hg). The sheet from which the specimens were prepared was rolled from small arc-cast buttons with the exception of TV-20, which came from a large arc-melted ingot.<sup>1</sup> All specimens were annealed at 900°C for one hour. It is seen that decreasing the titanium content and increasing chromium content improves the resistance to creep.

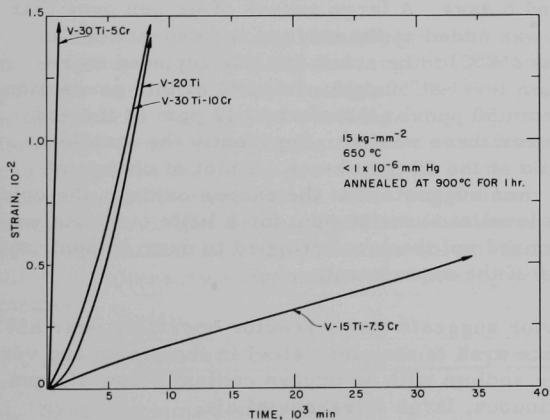


Figure 7  
Creep of Annealed V-Ti-Cr  
Sheet Alloys at 15-kg-mm<sup>-2</sup>  
Stress and 650°C

<sup>1</sup>Burt, W. R., Jr., Kramer, W. C., McGowan, R. D., Karasek, F. J., and Mayfield, R. M., Consolidation and Fabrication Techniques for Vanadium-20 w/o Titanium (TV-20), ANL-6928 (Feb 1965).

Strain-time curves for biaxially stressed tubular specimens of TV-20 at 600°C and 650°C are shown in Figure 8. In these tests the longitudinal strain was entirely elastic, and only plastic hoop strain was measured after unloading the applied stress. Both specimens were given a one-hour annealing heat treatment at 900°C before testing, and both were biaxially stressed with an internal gas pressure (argon) at a hoop stress of 15 kg-mm<sup>-2</sup>. The short duration of second stage creep at 650°C as compared to 600°C is clearly evident. The corresponding minimum creep rates are in the ratio of 3.2 to 1. The longitudinal strain at both temperatures was very low (<0.08%).

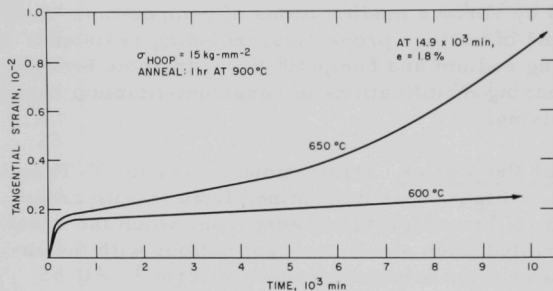


Figure 8  
Creep Behavior of Annealed  
V-20 w/o Ti Alloy

(ii) Corrosion of TV-20 in Sodium Containing 50 ppm of Oxygen. Corrosion loss versus time for TV-20 in sodium (containing 50 ppm by weight of oxygen) at 650°C was studied with individual samples exposed for 1, 2, 3, 4, 5, and 6 days. A large excess of oxygen over that required by the specimens was added at the start of the experiment and stored in the "cold trap" (at 250°C) to be automatically supplied as required to maintain the oxygen level at 50 ppm. In spite of this precaution, the oxygen level dropped from 50 ppm at the start to 18 ppm at the end (total duration of test was over three weeks). Apparently the stainless steel reacted with the oxygen at the 50 ppm level. A plot of change of thickness of TV-20 versus time suggests that the excess oxide in the cold trap maintained the oxygen level at about 50 ppm for a little over one week. At this time, the oxide was used up, the level dropped to near 20 ppm, and remained there for the rest of the experiment.

This behavior suggests that a reactor operating near 650°C with the typical large surface area of stainless steel in the piping and vessel, would of necessity have sodium with an oxygen content below 20 ppm, except if there were a continuous, large inleakage of air.

## 2. Condition of EBR-II Core-I Fuel

A group of EBR-II "special" fuel rods are being examined following each 0.25 a/o burnup interval. The special rods are ordinary Core I rods

that have received more thorough and careful dimensioning and testing before irradiation. It was hoped that postirradiation measurements would yield precise data concerning changes that take place in the U-5 w/o Fs fuel alloy with the steadily increasing exposures.\* These data will be compared with results obtained previously from capsule irradiations in thermal reactors. The first group of seven special rods were irradiated to 0.26 a/o burnup in the central positions of subassembly C140 located in reactor row 2.

Measurements of diameter and length disclosed only small changes (see Table VIII). The change in the volume of the clad fuel rod as measured by immersion was also very small.

Table VIII. Results of Examination of EBR-II Core-I Special Fuel Rods after 0.26-a/o Maximum Burnup

Rod No.	A9	A12	A8	A11	A14	A10	A13
Clad Fuel Rod:							
Length Increase, %	0.054	0.054	0.047	0.046	0.058	0.041	0.045
Diameter Increase, %	0.69	0.46	0.34	0.40	0.57	0.63	0.11
Volume Increase, %	-	-	-	0.22	-	0.22	0.07
Bare Fuel Pin:							
Length Increase, %	0.14	0.12	0.05	0.16	0.07	0.11	0.15
Diameter Increase, %	0.41	0.28	0.28	0.07	0.07	0.28	0.14
Volume Increase, %	0.60	0.61	0.53	0.69	0.61	0.66	0.60

The stainless steel cladding was removed in a decanner, which cut the cladding spirally along the length of the rod and then unwound it to expose the sodium-covered fuel pin. The sodium was removed by reacting with alcohol. Samples of cladding from regions of high exposure were retained for bend testing and structure examination. Length and diameter changes of the bare fuel are shown in Table VIII. Maximum length deviation from the preirradiation value was 0.6 mm (0.024 in.) and the maximum diameter deviation (from 18 postirradiation readings on each pin) was 0.02 mm (0.0008 in.). The average volume increase of the bare fuel was 0.61%. Volume measurements were made by the immersion-buoyancy method.

## F. General Fast Reactor Fuel Reprocessing Development

### 1. Skull Reclamation Process

Pilot-plant studies of the skull reclamation process on a scale of 1.5 kg of uranium are nearing completion. The development of plant-size (~4.25 kg U), remotely operated equipment is underway.\*\*

\*Work relating to the development of plant-scale processing equipment for the skull reclamation process was previously reported in another subsection (Fuel Cycle Facility for EBR-II) of this report. This work will now be included as a part of this subsection.

During the past month, an alternative flowsheet (see Figure 9) was investigated in the pilot plant. This flowsheet provides considerable simplification, both in process and equipment operation. In the step following the noble-metal-extraction step, an early step in both flowsheets, uranium oxide suspended in the molten salt phase is contacted directly with a magnesium-rich solution (60 w/o Mg-Zn). As the oxides are reduced, metallic uranium precipitates almost completely in the reducing alloy. After the reduction is complete, both the metal supernatant and the flux are discarded as waste. The precipitated uranium is redissolved in a Zn-14 w/o Mg solution and the product solution is transferred to the re-torting operation.

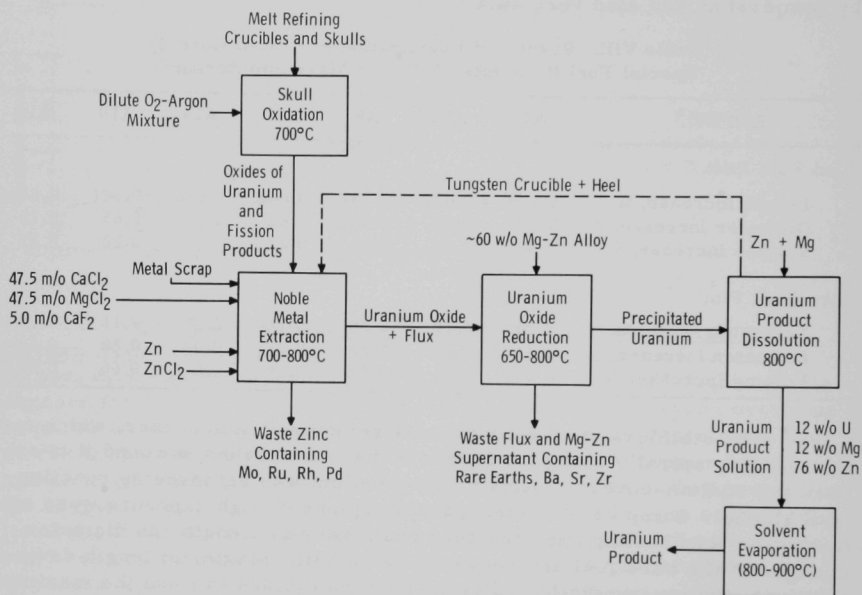


Figure 9. Alternative EBR-II Liquid Metal Process for Reclamation of Melt Refining Skulls

This alternative flowsheet offers a number of important advantages: (1) Two steps (the intermetallic precipitation and decomposition steps) are eliminated, thereby shortening the flowsheet. (2) Operating time is reduced by about a factor of two or three. This is brought about not only by the shortened flowsheet, but also by eliminating temperature cycles which, in the original flowsheet, required considerable time to effect. Once the equipment is at temperature, it should be easily possible to process a batch of material within 8 hr. (3) Equipment operation is simplified. (4) Reagent consumption and waste volumes are substantially reduced. (5) Uranium

recovery is increased (the uranium loss has been shown to be less than 1% as compared with uranium losses of 2 to 3% by means of the former flowsheet). (6) For equipment of the same size, process batch sizes may be increased by 60 to 100%.

To demonstrate this alternative flowsheet, two runs were carried out with charges composed of skull oxide, ceric oxide, and zirconium oxide. No operational difficulties were encountered and uranium recovery was near 100%. Consideration of the alternative process indicates that the removal of fission products, with perhaps the exception of zirconium, will not be affected adversely by substituting the alternative flowsheet for the earlier flowsheet. Removal of zirconium by the alternative process is being studied.

a. Skull Reclamation Run in Plant-scale Furnace. In the first skull reclamation run in a plant-size furnace (Run SRR-1), conditions of the original flowsheet<sup>2</sup> were followed. However, since fission product elements were not present in the skull oxide, the noble-metal-extraction step was eliminated, and the run was started at the reduction step. The feed material was 5.0 kg  $U_3O_8$  (4.25 kg U). The uranium oxide suspended in the flux phase was reduced at 800°C to uranium metal by the magnesium present in an approximately Zn-5 w/o Mg alloy. The charging, heating, mixing, and sampling operations were performed satisfactorily.

In this first run, a relatively low mixing speed of 400 rpm was used to provide the initial data on the relationship of mixing speed with rate of uranium reduction. The reduction was 87% complete in 1 hr and 93% complete in 4 hr. This rather low reduction rate can undoubtedly be increased by an increase of the agitation intensity.

Successful transfers were made of metal and flux after the reduction and uranium-precipitation steps. After the reduction step, 94% of the Zn-5% Mg supernatant solution was removed. After the uranium precipitation step, 93% of the available Zn-50 w/o Mg solution was removed. The overall transfer of flux in the two steps was about 98%, with 92% being transferred in the first step and 6% in the second step.

The final uranium product solution could not be transferred from the process crucible because of the failure of several heaters in the heated section of the transfer line. The transfer line was subsequently rebuilt and reinstalled in the furnace. The uranium-zinc-magnesium product was remelted and transferred from the crucible. On the basis of overall material balance, 98% of the uranium product was transferred.

The above transfer efficiencies are considered to be very satisfactory.

---

<sup>2</sup>Chemical Engineering Division Research Highlights, May 1964-April 1965, ANL-7020, p. 17, Figure I-7.

## 2. Pyrochemical Processes for HTGR and Other Reactor Fuels

The processing of carbide fuel ( $\text{ThC}_2$  and  $\text{UC}_2$ ), such as from the High Temperature Gas Cooled Reactor (HTGR), by means of a nonaqueous process flowsheet is being investigated. A conceptual flowsheet has been developed which makes use of fluid-bed and pyrochemical processes for the purification and recovery of the fuel material and for its reconversion to the final carbide form. In the first steps of the flowsheet, fluid-bed oxidation and chlorination of the spent fuel are carried out. Next, the pyrochemical steps of the process are employed. These consist of selective reduction of the chlorides of elements more noble than uranium and thorium (e.g., Mo, Ru, and Pd) by cadmium or a cadmium-zinc alloy. The noble fission products are extracted into the metal phase, which is then discarded as waste. Subsequently, the uranium and thorium chlorides are reduced by contacting with a magnesium-cadmium solution. The bulk of the rare earth elements remain in the salt phase, while most of the uranium and thorium transfer to the metal phase. A countercurrent extraction operation will be used to achieve both a high recovery of uranium and a high removal of rare earth elements.

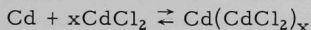
In order to determine the feasibility of the pyrochemical steps, a run was made in which batch extractions were employed, instead of batch countercurrent or continuous countercurrent extractions, to obtain information on the distribution coefficients and to indicate the possibility of achieving the desired results in a countercurrent operation. In the run, a change was made in the noble-metal-extraction step, which, in the conceptual flowsheet, involves the reduction of the noble elements from a salt solution. In simulating this step, uranium, thorium, and cerium were oxidized by  $\text{CdCl}_2$  from a Cd-3 w/o Zn solution containing thorium, uranium, cerium, and molybdenum. Cerium was used as representative of the rare earth elements and molybdenum as representative of the noble elements. The end result should be independent of whether thorium, uranium, and cerium in metal solution are oxidized and transferred to a salt solution or noble metals, e.g., molybdenum, in a salt solution are reduced and transferred to a metal solution.

From the results of this run, the following conclusions were made:

- (1) Selective oxidation of uranium and thorium from metal solutions and transfer to a salt solution can be accomplished smoothly. The alternative reduction of noble metal chlorides into a metal phase would be expected to go equally well. Excellent separation of uranium and thorium from noble metals is possible.
- (2) Distribution coefficients for uranium, thorium, and cerium are such that high recovery of uranium and thorium, and excellent separation from rare earths and alkaline earth elements, can be achieved in a relatively small number of extraction stages.

(3) The pyrochemical steps should be easy to perform by the use of either batch or continuous operations.

A cadmium-based flowsheet for the processing of high-plutonium breeder fuels is also being investigated. Cadmium-magnesium solutions are being considered for use as the liquid-metal solvent. One step of the process involves the rechlorination of cadmium metal in the presence of molten salt (consisting of mixtures of alkali and alkaline earth chlorides) to regenerate  $\text{CdCl}_2$  which serves as an oxidizing agent. In this chlorination step, a lower-valent cadmium chloride has been observed and is being investigated. The reaction



is being studied by equilibrating liquid cadmium with  $\text{CdCl}_2$  in molten  $\text{LiCl}$  at  $650^\circ\text{C}$ . Spectrophotometric measurements indicate the value of  $x$  in the above equation to be 2 within the experimental uncertainty. Further work is being done in an effort to determine the equilibrium constant for the reaction.

### 3. Decladding Studies for TV-20 Cladding

Although mechanical decladding is used for the present EBR-II fuel, this method may not be feasible for high-performance metal fuels because extensive irradiation is likely to cause metallurgical bonding between the fuel and the cladding. Therefore, a hydriding method for separating the fuel from the cladding is being investigated (see Progress Report for January 1965, ANL-7003, pp. 22-23).

Earlier studies had led to the conclusion that U-Fs and U-Pu-Fs alloys clad with TV-20 (vanadium-20 w/o titanium alloy) could be hydrided by diffusion of hydrogen at 2 to 3 atm pressure through the cladding (see Progress Reports for November 1964 and January 1965, ANL-6977, pp. 25-26, and ANL-7003, pp. 25-26). A more definitive experiment was recently performed with a U-15 w/o Pu-10 w/o Fs pin clad with TV-20 which had been welded, sodium bonded, and leak tested by the standard procedures used in the fabrication of fuels. No hydriding of the clad pin occurred under 2 to 3 atm hydrogen pressure at temperatures from 200 to  $425^\circ\text{C}$ . However, when a 1/16-in. hole was drilled in the cladding above the fuel, hydriding occurred, with complete disintegration of the pin and fragmentation of the cladding. The extensive hydriding observed in the earlier experiments with fuel pins enclosed in vanadium-titanium alloy is now attributed to incomplete sealing of the cladding alloy, which permitted hydrogen to gain access to the pin. No further development of this decladding method is planned until a specific need arises.

#### 4. Materials Evaluation

a. Corrosion Resistance of Iron-Chromium Alloys. One of the processes currently under development for the recovery of high-plutonium breeder reactor fuels utilizes cadmium and halide salts. Magnesium and zinc are added to the cadmium during the process to produce desirable solubility effects. In earlier work, Type 405 stainless steel was found to possess adequate resistance to corrosion by the process solutions and, therefore, to merit consideration as a material of construction for this process (see Progress Report for April 1965, ANL-7045, p. 23). However, other alloys are also being tested for this application in an effort to find a less expensive metal and one which could be more easily fabricated into equipment parts. Testing for corrosion resistance of three iron-chromium alloys: (1) Type 430 stainless steel (14-18% chrome-ferritic steel), (2) Type 1-SR steel (410 stainless steel with 3% aluminum addition), and (3) Type 7-Mo steel (Type 329 stainless steel) was continued (see Progress Report for May 1965, ANL-7046, p. 33). Another screening run was conducted at 650°C for 24 hr in an 81 w/o Cd-11 w/o Zn-6 w/o Mg-2 w/o U/ chloride salt system. Of the three alloys tested, Type 430 stainless steel appears to be the most promising for this application. A corrosion rate of <0.5 mil/day was obtained. Additional testing of this alloy is planned.

#### 5. Burnup Analysis--Neutron Activation Analysis by the Use of an Internal Flux Monitor

To date, two methods have been established for the determination of burnup on EBR-II fuel. In one, technetium-99 is determined spectrophotometrically; in the other, lanthanum-139 is determined by mass-spectrometric-isotope-dilution analysis. Although each of these methods is quite satisfactory for the present EBR-II fuel, other methods may be required for other EBR-II fuels. A program with the dual purpose of obtaining fission-yield data and developing other burnup methods is presently being pursued.

Neutron activation analysis is being investigated for possible application to burnup analysis. By incorporating a novel technique which we have chosen to term the "internal flux monitor," the accuracy of neutron activation analysis has been improved from the usual  $\pm 10\%$  to  $\pm 1\%$  (R.S.D.). This marked increase in accuracy is achieved by eliminating all need for knowledge of the flux intensity, the flux attenuation by the sample, and the duration of the irradiation. The technique incorporates into neutron activation analysis the same general aspects of the internal standard technique used in X-ray fluorescence analysis.

The internal flux monitor (IFM) technique consists of adding a known amount of element A to a solution containing an unknown amount of element B, irradiating the mixture, and measuring the induced activities. The activity

ratio obtained for the "unknown" mixture is compared with the activity ratio obtained with a solution containing known amounts of elements A and B.

The reasons for the significantly improved accuracy when using an IFM in neutron activation analysis can be seen from the following equation. For short irradiations the activity of an element after irradiation is given by the equation

$$\frac{dN}{dt} = \lambda N \sigma \phi t, \quad (1)$$

where

$dN/dt$  = activity of the nuclide produced;

$\lambda$  = decay constant of the nuclide produced;

$N$  = atoms of the original nuclide present at the start of the irradiations;

$\sigma$  = cross section of the original nuclide;

$\phi$  = neutron flux;

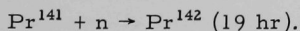
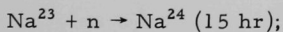
$t$  = time of the irradiation.

The activity ratio resulting from the irradiation of elements A and B can be written:

$$\frac{dN_A/dt}{dN_B/dt} = \frac{\lambda_A N_A \sigma_A \phi t}{\lambda_B N_B \sigma_B \phi t} = K \frac{N_A}{N_B}, \quad (2)$$

where  $K$  is a constant that can be measured accurately.

The IFM technique is being investigated for the analysis of praseodymium, with sodium as the internal standard. The neutron reactions are



After the irradiation, sodium is separated from praseodymium by carrying the praseodymium on a lanthanum hydroxide precipitate. Three precipitations are sufficient to achieve complete separation of the sodium-24 and praseodymium-142 activities. The precision attainable by the IFM technique was determined by simultaneously irradiating "unknown" and known praseodymium-sodium mixtures. Three irradiations were performed.

Each large irradiation capsule contained 4 smaller capsules: 2 unknowns and 2 knowns. A precision of 0.8% (R.S.D.) for a single unknown was obtained.

The internal flux monitor technique will also be applicable to the determination of burnup by lanthanum-139 analysis. Many aspects of the IFM approach are superior to the presently used mass spectrometric method. Other applications being considered are the analysis of binary mixtures of alkali metals, binary mixtures of the halides, as well as other pairs of elements which are particularly difficult to determine by more conventional analytical techniques.

## II. GENERAL REACTOR TECHNOLOGY

### A. Experimental Reactor and Nuclear Physics

#### 1. In-core Fast-neutron Spectroscopy

A fast-neutron spectrum was determined for ZPR-6 core No. 4Z by essentially the methods outlined in Progress Report for September 1964, ANL-6944, p. 53. Proportional counter probes filled with gases containing hydrogen were placed within the core material and the pulsed-height distribution of ionization from recoiling protons was observed.

Background ionization from gamma radiation was rejected from the distribution by means of pulse-shape discrimination. Spectra were recorded by two counters in succession; one contained essentially hydrogen and was used over the energy interval from 1 to 100 keV; the other contained essentially methane was used from 100 keV to 1 MeV. Improvements in experimental technique allowed improved statistics on recoil-proton distributions and more rapid extraction of a neutron spectrum from the experimental data.

The spectrum near the center of the core is shown in Figure 10; the composition of this central region is given in Table IX. Fine structure appears in the spectrum near 45 keV, which may be a consequence of the

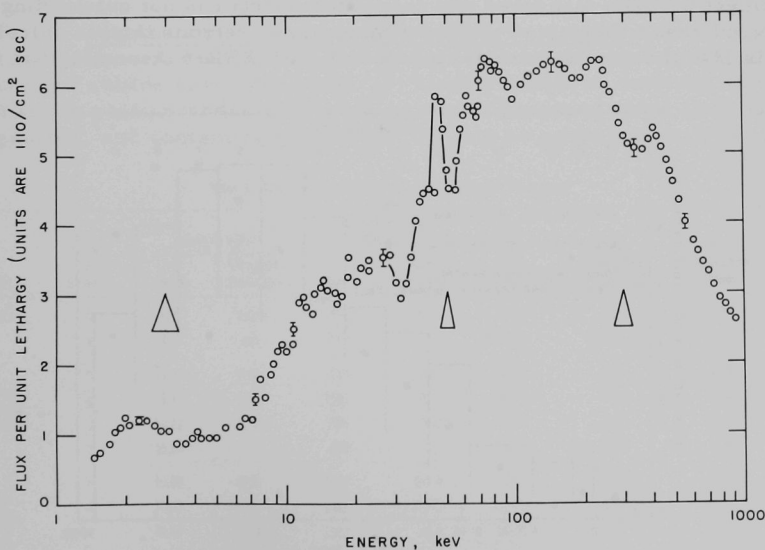


Figure 10. Neutron Spectrum at the Core Center of ZPR-6 Assembly 4Z. Triangles indicate detector resolution.

Table IX. Atomic Densities for  
ZPR-6 Assembly No. 4Z

Element	Atoms/cc $\times 10^{-24}$
$U^{235}$	0.00153
$U^{238}$	0.01062
Sodium	0.009258
Carbon	0.01290
Iron	0.009042
Chromium	0.002386
Nickel	0.001130

nonhomogeneous nature of the detector environment. A systematic error of 20% or so exists in the spectrum at 1 MeV due to wall and end effects, but this error decreases rapidly with decreasing energy.

Figure 11 is a comparison of the measured results with a group calculation [MAIM-6 using homogenized cross sections (Cross Section Set No. 801), ELMOE-averaged over the actual material concentrations.] The agreement between measured and calculated spectra is not outstanding; the measured result indicates relatively more slow neutrons than is calculated. This is also the result observed previously with ZPR-6 Assembly No. 3.

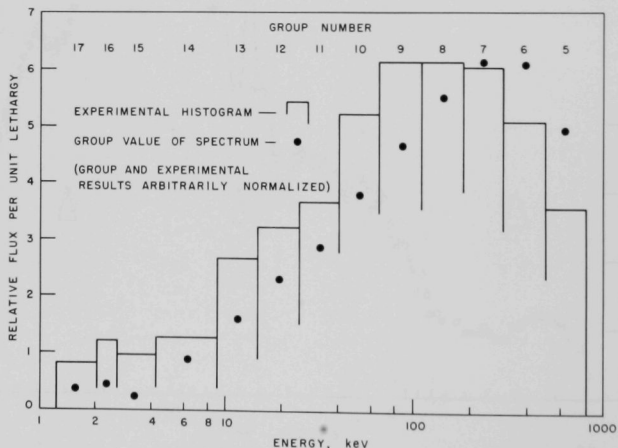


Figure 11. Comparison of Experimental and Group Calculation of Spectrum (Arbitrarily Normalized) at Center of Core for ZPR-6 Assembly No. 4Z.

## B. Theoretical Reactor Physics

### 1. Optimal Control of a Nuclear Reactor

For the development of large nuclear reactors, the spatial distribution of the flux inside the reactor core must be considered. The controlled variable is the neutron flux  $\Phi(s, t)$  which is a function of space  $s$  and time  $t$ . The excess reactivity, which is the control input, is also a function of space and time. We have determined this function in a form suitable to be realized as a closed-loop, automatic-control system. The approach used was quite general and can be applied to systems represented by a set of partial differential equations with spatial Hermitian operators.

## C. High-temperature Materials

### 1. Ceramics

a. (Th-U) Phosphides. A series of tests are being conducted to determine the flexural strength of uranium phosphide at various temperatures. Specimens were made by ball milling the UP for 5 hr, adding 1% stearic acid as a binder, and dry pressing at  $1400 \text{ kg/cm}^2$ . The bars measured 6.4 mm wide by 57 mm long, and slightly less than 6.4 mm in thickness. After firing in vacuum at  $1800^\circ\text{C}$  for  $2\frac{1}{2}$  hr, the bars had an average density of 94% of the theoretical value

b. Mechanical Properties of Uranium Compounds. Results of mechanical tests with uranium sulfide and phosphide are presented in Table X. Two batches of sulfide have been used: (1) freshly prepared material containing UOS in the grain boundaries, and (2) material prepared some time ago, homogenized, and containing particulate  $\text{UO}_2$  but no grain boundary film. The

Table X. Mechanical Tests of Uranium Sulfide and Phosphide

Material	Number of Samples	Density (g/cc)		Maximum Stress (kg/cm <sup>2</sup> )		Mean Load Rate (g/sec)	Mean Strain Rate (mm/sec x 10 <sup>4</sup> )	Total Deflection (mm)	Temp (°C)
		Mean	Standard Deviation	Mean	Standard Deviation				
Phosphide	5	9.7	0.005	1234	46.1	213.2	0.62	0.20	R.T.
	4	9.67	0.01	1556	198.2	195.0	0.58	0.27	1000
Sulfide Containing UOS Coarse Grain Size	5	10.09	0.04	529	20.3	303.9	1.17	0.14	R.T.
	4	10.12	0.015	1201	43.1	186.0	0.51	0.22	1000
	3	10.21	0.02	895	55.3	59.0	1.07	1.27	1250
	2	10.09	-	444	-	31.7	1.37	2.54	1500
Sulfide with No Fine Grain Size	4	10.65	0.01	1069	155.9	258.6	0.69	0.18	R.T.
	4	10.65	0.05	1215	189.1	213.2	0.61	0.23	1000
	4	10.67	0.01	1382	44.9	195.0	0.58	0.25	1250
	2	10.68	-	864	-	249.5	1.14	2.54	1500

phosphide batches were freshly prepared, and the quality improved with experience in pressing and sintering the bend test bars.

Heating sulfide containing UOS to 1000°C increased the strength by a factor of two over the value at room temperature, but the strength decreased again with further rise in temperature. At 1500°C the strength was less than that at room temperature. Ductility rose slowly up to 1000°C, and then very rapidly at higher temperatures. At 1500°C, the material was extremely plastic and flowed readily at low loads.

Sulfide without UOS was much tougher. The strength rose with increase in temperature up to 1250°C and fell at 1500°C, although at this temperature it was twice as strong as material containing UOS. The ductility rose slowly to 1250°C, then very sharply at 1500°C, at which temperature the material was highly plastic. Bars were easily deflected to the limit of the bending tools (2.5 mm) without cracking.

Phosphide was stronger than the strongest sulfide, and increased in strength at 1000°C more than sulfide. The ductility remained slightly higher than sulfide. Tests so far have not exceeded 1000°C with this material.

The effect of temperature on ductility of these compounds with the rock-salt crystal structure is more sudden and at an increasing rate, compared with  $\text{UO}_2$ , which has the fluorite structure. Indications are that phosphide will be stronger than  $\text{UO}_2$  below 1500°C but not above. Sulfide without UOS is very similar to  $\text{UO}_2$  below 1500°C.

The mechanism of deformation at room temperature appears to resemble that of  $\text{UO}_2$  by expansion of voids, leading to crack information, in specimens of phosphide and sulfide examined so far.

c. Anelasticity of Some Uranium Compounds. The investigation of the effect of density, grain size, and oxygen/uranium ratio on the elastic modulus and internal friction of uranium oxide has continued. The values obtained when the density and grain size were varied confirmed previous results (see Progress Report for May 1964, ANL-7046, pp. 47-48). The modulus increased as the density increased and the internal friction was larger as the grain size decreased. In the study of the effect of grain size, care was taken to maintain constant the density and stoichiometry of the specimens. The only other parameter that varied during preparation of the specimens was the porosity, meaning by that the number, size, shape, and distribution of pores.

In the study of the effect of the oxygen/uranium ratio on the elastic modulus and on the internal friction of uranium oxide, the decrease of the elastic modulus started to level off at an O/U ratio of about 2.07.

Furthermore, the amplitude of vibration at resonance became smaller, owing to the increase in the values of internal friction.

Assembly of the furnace for the measurements at higher temperature has started.

d. Uranium-mixed Anion System. Studies of the system UP-US have continued. Samples have been prepared at 10 w/o intervals across the system, and have been fired at 1800°C and 2000°C in vacuum. US shows a greater weight loss than UP, and the intermediate compositions generally exhibited weight losses that fell between those of the end members. The two compounds are completely mutually soluble across the entire compositional range, and a plot of lattice constants versus composition shows a slight positive deviation from linearity.

Solid-solubility studies of binary systems among the compounds UN, UC, US, UP, and UAs were conducted. The extent of solubility among the compounds appeared to be mainly a function of the size differential between the nonmetal atomic radii. Substitutional solid solutions of extensive range resulted only when the radii of the solvent and solute atoms did not differ by more than 14%. Where solid solution was restricted and the non-metal atom size differential was the same, there appeared to be greater solubility when the solvent atom was larger than when it was smaller. Valency factors did not appear to affect solubility among the NaCl-type uranium compounds, as they did among metals. Solid solubility among these uranium compounds followed closely the size factor rules found by Hume-Rothery for metals and those observed among refractory monocarbides by Norton and Mowry.

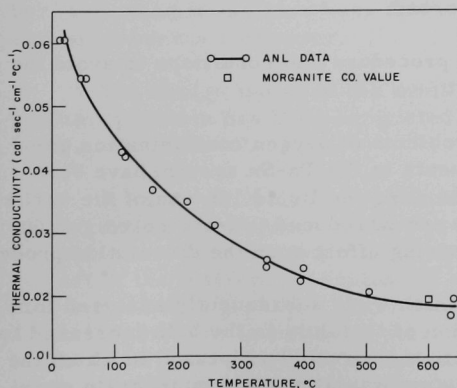


Figure 12. Thermal Conductivity of Aluminum Oxide

e. Development of Thermal-diffusivity Rig for Ceramic Materials. An experimental technique for obtaining thermal-conductivity data on nonconducting ceramics over a temperature range has been developed and checked with Triangle RR aluminum oxide, as shown in Figure 12. The value given by the Morganite Company for this material at 600°C falls on the curve obtained at ANL.

The glovebox in which this equipment is situated has been closed and studies on plutonium ceramics are in progress.

## 2. Liquid-Metal Corrosion

a. Polarization Studies. Continued investigation accounted for the lowering of film resistance on a pre-oxidized zirconium surface in a sodium vapor-phase region of the polarization cell, for approximately one centimeter above the liquid-vapor interface (see Progress Report for May 1965, ANL-7046, p. 49). The effect occurred during overnight exposures of unalloyed zirconium rod electrodes to oxygenated sodium at a central sodium temperature of 540°C. Electrodes extend from the central melt region upwardly through the melt surface into a volume containing sodium vapor and argon cover gas, and then through insulated seals to the cell exterior. A temperature gradient typically exists along an electrode except in the central sodium. Vapor-phase sample sections were preoxidized to avoid condensate interference in the vapor region.

Lowering of film resistance near the liquid surface was thought to be due to one or more of the following: a) a cover-gas impurity, such as moisture; b) a sodium-condensate effect; or c) partial dissolution of film by the zirconium. Cold trapping the argon cover-gas supply line to remove moisture did not eliminate the effect, nor did the deliberate production of an oxide crust on the melt surface, to inhibit vaporization of sodium. It was also shown previously that local heating of the electrode in the region of the effect (to avoid sodium condensation) did not prevent resistance loss. However, holding an oxidized electrode in vacuum environment at 520°C overnight produced a similar lowering of film resistance. Thus it appears that dissolution of film by zirconium may lower the surface resistance without substantial change in film appearance, perhaps because of uneven thickness of the original film. The effect was less or absent farther from the melt because of lower temperature, and was absent in the melt because of readily available oxygen to make up that absorbed.

Various modifications of procedure and conditions to avoid the effect are being considered.

b. Dissolution Kinetics. Problems of oxygen contamination encountered during dissolution experiments in the Ta-Sn system have been solved by improving the method of sampling the liquid. In one of the earlier runs, trace amounts of oxygen (air) were introduced into the cover gas during the sampling procedure, with the following effect upon the dissolution process:

The liquid-tin samples, which were subsequently analyzed for tantalum, showed that the concentration of tantalum in the bath increased to about 50% of the saturation concentration over the 8-hr period in which the samples were obtained. When the system was allowed to equilibrate overnight, during which time no additional oxygen was admitted to the system, subsequent samples showed that the bath had reached saturation. The tantalum disc at the conclusion of the run was found to have decreased uniformly in thickness, and the weight loss was greater by a factor of ten than that required to saturate the isothermal tin reservoir.

These results tend to indicate that oxygen prevents the system from reaching saturation by oxidizing the tantalum from solution at or near the liquid-gas interface. The dissolution process at the tantalum disc-liquid interface proceeds at a rate that is related to the difference between the saturation concentration and the steady-state concentration of tantalum in the tin reservoir. The later quantity is determined by the rate of dissolution of the disc and the rate of oxidation of tantalum from the system.

The uniform dissolution of the disc is additional confirmation of the concepts upon which these experiments are based.

X-ray diffraction patterns obtained from samples of the tin melt indicated that a large amount of  $Ta_2O_5$  was present along with the tantalum.

Recent runs have yielded smooth dissolution curves in which the times required to reach saturation are less than 4 hr. More experimental data are required to determine the effects of hydrodynamic conditions on the dissolution process. The pertinent experiments are in progress.

c. Zirconium Alloys for Superheated Steam. This program is complete and experimental work has been terminated.

### 3. Component Surveillance Loop

A loop is being constructed to test component parts, such as valves, in high-temperature flowing sodium. Construction of the electromagnetic pump is about 60% complete. The magnet, copper conductors, compensating bar, and other items have been fabricated. The copper bus bar is being shipped from the fabricator.

The design layout of the modified wear-testing device for 1200°F sodium operation has been completed. Portions of the mechanism are being purchased.

A water-analysis meter for continuous recording of blanket-gas water content was received from the Consolidated Electrodynamics Corporation. This unit will be installed in the loop blanket-gas system as part of the instrument-evaluation program. Initial tests of this device with argon bottle gas show water contamination levels of the order of 2.5 to 5 ppm. The insertion of plastic tubing raises the water contamination levels to 30 ppm. These observations point to the necessity for proper inert gas-system installation to preclude the introduction of contaminants into a blanket gas. It also demonstrates the need for constant monitoring of gas installations for possible compromise of purity.

#### 4. Irradiation Testing

a. Transient Irradiations of Plutonium Carbide. Three jacketed specimens of vibratorily compacted PuC, each contained in a graphite-lined stainless steel capsule, were subjected to elevated-temperature transients in the TREAT reactor. Data are tabulated in Table XI. The specimens, jacketed with nominal 0.23-mm (0.009 in.) thick Nb-1 w/o Zr or Type 304 Stainless Steel tubing, had not been previously irradiated. Measured jacketing temperatures ranged from 773 to 1434°C.

Table XI. Reactor and PuC Specimen Data for Metallurgy  
TREAT Experiments 4-1 through 4-3

Metallurgy Experiment No.	Transient No.	Specimen No.	Jacket Material	Integrated Reactor Power (MW-sec)	Maximum Temp <sup>(a)</sup> (°C)
4-1	818	F-9	304 SS	29.2	1434
4-2	819	C-40	Nb-1 w/o Zr	13.2	901
4-3	820	C-41	Nb-1 w/o Zr	21.2	1208

(a) The temperatures are the maximum recorded jacket surface temperatures. Each jacket had three thermocouples attached.

The results of the post-transient examination revealed that the integrity of the Nb-1 w/o Zr jacketed specimens had been maintained. There were no dimensional or volume changes of significance. Each specimen had three thermocouples attached to the jacket surface at widely separated points, and these indicated a nonuniform temperature distribution along the specimen during the transient. The specimen jacketed with Type 304 Stainless Steel failed in a nonviolent fashion. An examination of the plutonium-carbon phase diagram indicated that in this instance (42.3 a/o C) liquid-phase plutonium would exist at temperatures above 900°C. Since plutonium and iron form a low melting eutectic, the failure is not unexpected.

Analysis of the specimen temperature traces obtained during the transient indicate that approximately 2.7 sec elapsed between the time molten plutonium came in contact with the jacket and the time jacket failure occurred. At the time of failure, jacket temperatures ranged from 987 up to 1377°C. Metallographic examination of the specimens is planned.

#### D. Other Reactor Fuels and Materials Development

##### 1. Nondestructive Testing

a. Ultrasonic Instrument and Transducer Development. In the search for an improved backing material for ultrasonic transducer probes, pressed and sintered stainless steel appears promising. A vendor who

has the capability to fabricate stainless steel forms of various porosities has been contacted and appraised of our needs. Several cylinders of this material will be ordered and tested.

b. Development of a Neutron-image Intensification System. An intensifier tube and associated close-circuit television system has been set up in the Chemistry Division Hot Laboratory. Arrangement of a zoom lens on the television system makes it possible to present an image of about 4-mm-dia area on about one-third of the scanning lines. The anticipated image area at the neutron intensifier output screen will be about 4 mm when used with the presently arranged Cm-Be neutron source moderator-collimator.

c. Suppression and Reduction of Noise in Electromagnetic Test Systems. The problem of noise in general is the chief factor limiting the application of electromagnetic test systems to many nondestructive-testing problems that superficial consideration would indicate could best be solved by an electromagnetic method. In broadband test systems, noise generated within the test system itself can be a limitation on the useful sensitivity because the noise power available from many sources is proportional to the system bandwidth. Work has so far been concentrated on a study of this type of noise rather than noise originating in the test specimen.

A block diagram of a broadband test system of the type developed at ANL is shown in Figure 13. Most of the noise in such a system originates from three main sources:

- i. preamp noise (thermal and shot noise);
- ii. pulse-generator noise;
- iii. noise originating from time jitter in the sampling pulse.

Of these three, preamp noise is the most important source. The preamplifiers formerly used with these broadband test systems usually had a passband of from about 0.15 to 1.3 Mc at the 3-db points. A calculation of the bandwidth necessary to handle an idealized reflected pulse showed that the actual signal-to-noise ratio might be improved if the bandwidth were extended, particularly at the low-frequency end. This apparent contradiction occurs because a considerable amount of useful information carried in the pulse developed across the pickup by the resultant field outside the specimen was being lost due to bandwidth restrictions. This was confirmed experimentally by measurements made with amplifiers providing a passband from 0.05 to 1.7 Mc at the 3-db points.

Equipment was constructed and assembled to measure the preamplifier noise over the entire passband. Measurements showed that the preamps already in use had provided reasonable low-noise performance, but that considerable improvement was still possible. Lower-noise preamps have been designed and tested.

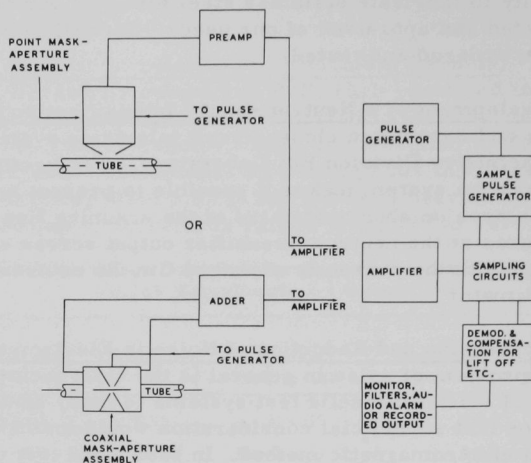


Figure 13. Block Diagram of a Pulsed Electromagnetic Test System

Pulse-generator noise is noise appearing as a modulation of the pulse height and is usually proportional to the pulse amplitude. At the present time the pulse-generator noise contributes about one-fourth as much noise power in the system output as the best preamp which has so far been built, but as the preamp noise figures improve (which is probable), generator noise will make an increasingly important contribution to the system noise. Unfortunately, relatively little of fundamental or quantitative nature is known about this so-called "large signal noise."

Noise originating from time jitter in the sampling pulses has the following origin. When sampling is used to retrieve information from the reflected pulse, a sampling pulse is stationed upon the reflected pulse waveform, and this elevated section becomes that part of the pulse which is passed through the rest of the system for further processing. The time when this sampling pulse occurs relative to the reflected pulse is variable, and when a time is selected during which the reflected pulse is changing amplitude rapidly, any jitter between the two pulses will generate a noise voltage at the system output. More stable sampling circuits have been designed that have nearly eliminated this problem, at least temporarily, but as quieter preamps are constructed, the problem may again require improvement.

The reduction of system noise can in itself effect an improvement in the signal-to-specimen noise ratio. As an example, if as a result of improvements in system signal-to-noise ratio, a doubling in the average mask-aperture-to-specimen spacing is permitted, it is obvious that

specimen noise due to a certain level of mechanical vibration of the specimen will assume less importance. A reduction in system noise to a state-of-the-art minimum seems a logical preliminary step before the more complicated subject of specimen noise is assaulted.

d. Infrared Systems for Nondestructive Testing. An indium antimonide infrared-detection system was used to inspect a sample of flat fuel plate with known nonbonds. The heat source was a 500-W infrared line heat lamp focused on the fuel sample at a fixed distance ahead of the detector. The fuel sample was moved at a constant velocity. The surface-temperature measurement is made by focusing the radiometer on a "detector spot." The detector spot is placed behind the heat line, causing a time delay in the temperature measurement. This delay allows the heat to diffuse into the cladding and reach the unbond, and so to cause excess temperature to appear at the surface. The initial tests indicate that the known nonbonds can be detected by the radiometer when a transient heating technique is used. The detector delay time and fuel-sample velocity are now being optimized.

e. Thermal Conductivity of Irradiated Fuel as a Function of Burn-up and Temperature. The thermal-pulse method of measuring thermal diffusivity and conductivity is being utilized to determine the thermal properties of irradiated fuel pins as a function of burnup. This method will enable the diffusivity and conductivity to be measured in both the axial and radial directions at many points along the fuel pin and, thus, will indicate any anisotropy in the thermal properties, as well as any variation of these properties in the axial and radial directions along the length of the fuel pin.

A room-temperature setup has been installed in a cave. Room-temperature measurements of the diffusivity and conductivity of the uranium-fissium alloys are being repeated. This will enable the operation of the system to be checked, and will serve to develop the facility necessary for operating the remote manipulators.

## E. Engineering Development

### 1. Two-phase Flow

a. Void Fraction--Pressure-drop Facility. This facility has been inoperative for the past four weeks (see Progress Report for May 1965, ANL-7046, p. 55). A new electromagnetic pump has been fabricated and will be installed before operation is resumed.

### 2. Boiling Liquid-Metal Technology

a. Niobium-1% Zirconium Loop. This facility is designed to investigate the heat transfer and two-phase flow characteristics of boiling sodium to a temperature of 2100°F, corresponding to a pressure of approximately 8 atm. Among the variables to be investigated are boiling

heat flux and temperature difference up to the critical-heat-flux occurrence, boiling and adiabatic two-phase pressure drop, vapor volume fraction, and boiling-stability parameters.

Construction is 90% complete. It is anticipated that the loop will be shipped from Pratt & Whitney-CANEL in early July.

The loop support-structure assembly is 95% complete. Vendor difficulties encountered in tantalum procurement have caused a delay in the shutter and reflector-assembly schedule.

Instrumentation procurement and assembly are progressing. The pressure transducers have been mounted on a vacuum chamber flange and the containing oven is nearly complete. The diffusion-bonding experiment has shown that the thermocouple assemblies will probably be difficult to remove after 200 hr above 2000°F.

The flowmeter-cooling assemblies, and the sodium- and argon-purification systems are being fabricated.

The automatic data-acquisition system has been ordered and will be received in early July. The computer routines for data analysis are being formulated.

The stator assembly for the electromagnetic sodium pump was mounted in position to accept the pump duct and insulation assembly. The blower, air duct, capacitors, autotransformer, and switchgear panel are now installed. All power, control, and instrumentation wiring are complete. The control panel for this equipment is nearly complete.

Some modifications were made to the air manifold to provide blowdown for the water-cooled baffle and diffusion-pump quick-cool line. An exhaust line was constructed to serve the vacuum-chamber roughing pump and the liquid nitrogen baffle discharge. After oil change in the mechanical pumps, the chamber pressure can be consistently reduced to the high  $10^{-4}$ -Torr level. The cryogenic baffle, liquid-nitrogen-level-control system, and the diffusion pump have been brought into operation for short periods of time, and pressures in the high  $10^{-8}$ -Torr region have been reached. Some further debugging of the equipment is necessary. A sensitive relay in the vacuum protective circuit failed and has been bypassed pending replacement. A number of spare parts for the vacuum equipment have been ordered.

The overall schedule has been delayed approximately eight weeks.

## b. Heater Experiments

(i) Thermal Radiation Heater Experiment. This experiment has been terminated and a report will be issued as ANL-7038, "A Liquid-Metal Heat Transfer Experiment."

(ii) Electron Bombardment Heater. The electron-bombardment-heated, sodium pool boiling experiment has operated for approximately 30 hr. Difficulties involving the support of the cathode have caused delay. Following repairs noted in the Progress Report for May 1965 (ANL-7046, p. 56), the system was degassed and operation continued. Operation was terminated after several days due to the melting of the flexible leads which allow for the expansion of the cathode. Heavier leads proved too stiff to allow for the elongation of the cathode caused by thermal expansion. New leads are being designed for sufficient flexibility and current-carrying capacity.

During the short-term operation of the electron-bombardment-heated boiler, heat fluxes to 20,000 Btu/hr-ft<sup>2</sup> were obtained. The sodium surrounding the anode was sufficiently subcooled so that no boiling occurred. Thermocouples in the anode wall recorded temperature variations ranging up to 8°F/sec during heating periods.

## 3. General Heat Transfer

### a. Heat Transfer in Double-pipe Heat Exchangers

(i) Liquid-Metal Cocurrent Turbulent Flow. As mentioned previously (see Progress Report for May 1965, ANL-7046, p. 56), application of a new liquid-metal heat exchanger design method will be very convenient once certain quantities are computed and tabulated over ranges of practical interest. The computations and tabulations of these quantities have been completed, and will be published in a future report on liquid-metal double-pipe heat exchanger design.

(ii) Countercurrent Flow. The new liquid-metal heat exchanger design method mentioned above applies to countercurrent flow also. The related quantities, however, are more difficult to obtain than for the cocurrent flow case because of the unusual mathematical aspects of the counter flow problem (see Progress Report for March 1965, ANL-7028, p. 57). Two procedures for obtaining these quantities have been formulated, and programing for exploratory computations with the CDC-3600 has begun.

## F. Chemical Separations

### 1. Fluidization and Volatility Processes

#### a. Recovery of Uranium and Plutonium from Low-enrichment Fuels

(i) Laboratory Support Work. Experimental evaluation of bromine pentafluoride as a selective fluorinating agent for uranium in uranium-plutonium fuel materials was continued (see Progress Report for May 1965, ANL-7046, pp. 57-58). It is expected that the reaction between  $\text{BrF}_5$  and mixtures of uranium and plutonium compounds will result in the conversion of uranium to volatile  $\text{UF}_6$  while plutonium is converted to nonvolatile  $\text{PuF}_4$ . Plutonium is recovered as  $\text{PuF}_6$  in a subsequent step by fluorination of  $\text{PuF}_4$  with fluorine.

A series of tests were performed to evaluate the effects of the presence of Zircaloy and stainless steel decladding products on the conversion of uranium to  $\text{UF}_6$  in reaction mixtures containing  $\text{U}_3\text{O}_8$ , alumina, and fission product oxides. The decladding products were prepared by reacting the cladding with a mixture of hydrogen fluoride and oxygen. The fluorination reactions with  $\text{BrF}_5$  were carried out at  $400^\circ\text{C}$  for 1 hr. In the absence of decladding product materials, 99.8% of the uranium was converted to  $\text{UF}_6$ . In tests in which Zircaloy or stainless steel decladding product was present, over 99.6% of the uranium was converted to  $\text{UF}_6$ . These results indicate that the presence of decladding products does not affect the removal of uranium from  $\text{U}_3\text{O}_8$  by  $\text{BrF}_5$  and support previous observations made on tests in which the uranium in the reaction mixture was present as  $\text{UF}_4$  and  $\text{UO}_2\text{F}_2$  (see Progress Report for April 1965, ANL-7045, p. 40).

(ii) Decladding and Fluorination. Development studies are being performed in a 2-in.-dia fluid-bed reactor to determine the conditions for fluorinating  $\text{UO}_2$ - $\text{PuO}_2$  pellets containing fission products that would result in a minimum retention of uranium and plutonium on the fluid bed of alumina particles. A run was completed in which a 2-in.-deep bed of  $\text{UO}_2$ - $\text{PuO}_2$  pellets was reacted by a two-step process: (1) a two-zone oxidation-fluorination step (see Progress Report for January 1965, ANL-7003, pp. 58-59) at  $450^\circ\text{C}$  for 3 hr, and (2) a recycle-fluorination step with 90 v/o fluorine at  $450^\circ\text{C}$  for 5 hr,  $500^\circ\text{C}$  for 5 hr, and  $550^\circ\text{C}$  for 10 hr.

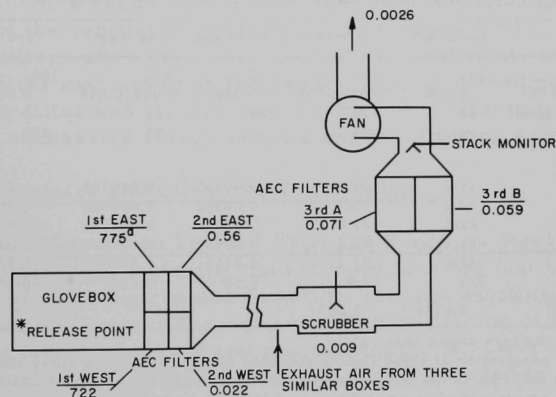
Plutonium analyses of bed samples taken at periodic intervals throughout the run indicated that the rate of plutonium removal during each recycle-fluorination period was the highest during the first two hours of each period. The overall plutonium removal during the run was 98.2%.

Nearly half of the alumina bed material was caked at the end of the run. The agglomerated material contained 0.0064 w/o plutonium; the plutonium content of the free-flowing alumina bed material was

0.0005 w/o. The extent of plutonium removal in the agglomerate suggests that the formation of the agglomerate may have occurred during the final recycle-fluorination period at 550°C. Several factors which may contribute to the agglomeration are being investigated: (1) diminution of the alumina particles by attrition and reaction, (2) the quality of fluidization during the recycle operation, and (3) local temperature excursions which might be produced by the high fluorine concentration at the onset of the recycle-fluorination step.

(iii) Cleanup of Cell Exhaust Air Contaminated with Plutonium Hexafluoride. On March 12, 1965, a 3/4-in.-dia fluorethene tube containing 5.7 g of  $\text{PuF}_6$  burst and the entire content of the tube was released into a ventilated glovebox. The release of  $\text{PuF}_6$  to the glovebox atmosphere was rapid, occurring over a time interval much less than the air-residence time in the box (5.8 min). Therefore, the occurrence was considered to be an instantaneous release. Although the release was accidental, it provided an excellent opportunity to study the containment of  $\text{PuF}_6$  in an alpha enclosure, especially since the glovebox and the glovebox filters had not been previously exposed to plutonium.

The ventilation air leaving the glovebox was filtered by two banks of filters in parallel; each filter bank contained two AEC filters in series. The filtered air passed through a scrubber and then through the stack filter (two AEC filters in parallel) before discharge to the building exhaust system (see Figure 14). As the gas passed through the final set of filters, a portion of the gas stream was sampled by a stack monitor



<sup>a</sup> THIS FILTER HAD TORN MEDIA NEAR THE CENTER OF THE FILTER

Figure 14. Schematic Diagram of the Ventilation System of the Glovebox. 5.7 g  $\text{PuF}_6$  released. Numbers give plutonium distribution in milligrams, after release.

containing an alpha counter which measured the activity of material deposited on an integral filter. A direct alpha count of the filter media indicated that the plutonium concentration in the exhaust gas averaged 300 MPC (maximum permissible concentration) during the short period (7 min) of discharge. The total quantity of plutonium discharged from the stack was estimated to be 2.6  $\mu\text{g}$ . All attempts to detect plutonium at monitoring stations downwind from the release stack failed to show any plutonium above normal background levels.

The plutonium distribution throughout the filtering system was determined in order to evaluate the performance of the air-cleanup system and to compare the performance with the results of small-scale release experiments which had been designed to simulate the large-scale releases. The filters were removed and sampled by cutting cores of the filter media with a thin-walled tube similar to a cork-boring tool. Four samples were taken from each filter by cutting cores from the center of each quadrant. Each core was unfolded and the filter media freed from the separators. The filter media from each core were leached with 250 ml of 10%  $\text{HNO}_3$  containing 0.03% wetting agent. The mixture was digested for 24 hr, and the solution filtered and analyzed for plutonium. A summary of the plutonium distribution on the filters is presented in Table XII. The total plutonium content of each filter is based on the inside cross-sectional area of the coring tool and the adhesive-free area of the filter. The distribution of plutonium throughout the filtering system is shown in Figure 14.

Table XII. Plutonium Distribution on AEC Filters after Release of 5.7 g  $\text{PuF}_6$

Filter	1st East <sup>a</sup>	1st West	2nd East	2nd West	3rd A	3rd B
Rated Flow (cfm)	135	135	135	135	1000	1000
DOP Penetration <sup>b</sup> (%)	0.008	0.004-0.005	0.008	0.004-0.008	0.018	0.018
Actual Flow Rate (cfm)	24	24	24	24	75	75
Area (sq in.)	94	94	94	95	472	468
<b>Pu Found (mg Pu)</b>						
Core I <sup>c</sup>	19.3	21.8	0.00155	0.000749	0.000346	0.000416
Core II <sup>c</sup>	23.4	19.4	0.00360	0.000568	0.000673	0.000294
Core III <sup>c</sup>	22.2	21.0	0.0597 <sup>a</sup>	0.000793	0.000327	0.000352
Core IV	21.4	22.1	0.00137	0.000499	0.000309	0.000318
Average	21.6	21.1	0.0166	0.000652	0.000413	0.000345
Total Filter	775	722	0.56	0.022	0.071	0.059
Pu Penetration (%)	0.073 <sup>a</sup>	0.0031	(20) <sup>d</sup>			2.0 <sup>e</sup>

<sup>a</sup>First east filter had torn media near center.

<sup>b</sup>Diethylphthalate penetration at rated flow, a standard test for evaluating filter efficiency.

<sup>c</sup>Sample core was 1.871 in. in dia and was removed from center of quadrant.

<sup>d</sup>This value could result entirely from a filter gasket leak of 0.003 sq in. in the gasket perimeter of 92 in. The value includes 0.009 mg Pu (7% collection) in scrubber between 2nd and 3rd filters.

<sup>e</sup>Filter discharge, based on analysis of the stack-monitor filter, was 0.0026 mg Pu.

The fraction of released plutonium which penetrated the AEC filters was within the range expected on the basis of results from the

small-scale release experiments<sup>3</sup> (see Table XIII). Comparison of these data indicates that the results obtained from the small-scale experiments can be used reliably to predict the behavior of large-scale releases.

Table XIII. Performance of AEC Filters during PuF<sub>6</sub>-Release Accident and Small-scale Experiments

	Accidental Release	Small-scale Experiments
PuF <sub>6</sub> Released (mg)	5700	1.5 to 25
PuF <sub>6</sub> /H <sub>2</sub> O <sup>a</sup>	0.006	0.022 to 3.32
Penetration of 1st Filter (%)	0.0031 <sup>b</sup>	0.0005 to 0.0016 <sup>c</sup>
Penetration of 2nd Filter (%)	2 to 20	2 to 45 <sup>c</sup>
Fraction of Released Pu Discharged from Last Filter	6.7 x 10 <sup>-7</sup>	10 <sup>-6</sup> to 10 <sup>-9</sup> <sup>c</sup>

<sup>a</sup>Average mole ratio in release enclosure volume due to moisture content of the contained air.

<sup>b</sup>Only west filter was considered since east filter had a torn medium.

<sup>c</sup>Only for experiments where PuF<sub>6</sub>/H<sub>2</sub>O < 0.1.

As a result of this investigation it became apparent that the performance of the ventilation system could be improved by: (1) in-place testing of the filters after each change of filters to indicate the presence of a flaw in the filter medium or in the gasket, and (2) providing a separate gasket for each filter and a more positive means of effecting the seal in the installation of successive filters in the glovebox filtering system.

## 2. General Chemistry and Chemical Engineering

a. Static Corrosion Tests of Type 304 Stainless Steel in Contact with Paste Blanket Materials. Mobile blanket materials for fast breeder reactors show promise of reducing reactor downtime for fuel shuffling, improving power-conversion efficiency through improved utilization of sodium coolant, and decreasing fuel-processing and fabrication costs. Development work in paste blanket fuels consisting of a ceramic fuel dispersed in a liquid metal has been carried out. The corrosiveness of such paste fuels toward possible container materials has been studied.

Static corrosion tests of Type 304 Stainless Steel of pastes prepared by mixing uranium mononitride, uranium dioxide, or uranium

<sup>3</sup>Chemical Engineering Division Summary Report, July, August, September 1962, ANL-6596, pp. 123-125 (1963).

monocarbide with sodium were made at 760°C. Type 304 Stainless Steel coupons, 5 mils thick, were immersed in the pastes which were contained in corrosion capsules that were also made of Type 304 Stainless Steel.

The tests lasted 1000 hr and results are given in Table XIV. Under the test conditions uranium nitride and uranium dioxide are compatible with Type 304 Stainless Steel. However, severe carburization occurred when the coupon was in contact with hyperstoichiometric\* uranium carbide paste and resulted in a marked increase in microhardness; in fact, the coupon fractured in several places while being mounted for metallographic examination. The carbon content of this coupon increased from 0.06 w/o to 1.6 w/o. Although such behavior is not unexpected with a hyperstoichiometric carbide fuel, recent reports indicate that carbon from hypostoichiometric carbide irradiated to a burnup of ~20,000 MWd/metric ton of uranium was transferred to its stainless steel sheath.<sup>4,5</sup> Static corrosion tests of pastes composed of sodium and hypostoichiometric uranium carbide in stainless steel are in progress.

Table XIV. Experimental Results of Static Corrosion Studies of 5-mil Coupons of Type 304 Stainless Steel in Contact with Sodium-Uranium Ceramic Pastes for 1000 hr at 760°C

Coupon	Contents of Capsule	Coupon Wt Change (mg/cm <sup>2</sup> )	Thickness Change (mils)	Metallographic Observations
1	Na	+0.03	0	Sensitized structure <sup>a</sup>
4	Na + Na <sub>2</sub> O (4000 ppm)	+0.4	+0.5	Intergranular corrosion
2	Na + UC (34 v/o) <sup>b</sup>	+0.9	+1	Heavy carbide precipitation throughout sample. Surface reaction layer visible.
5	Na + UO <sub>2</sub> (42 v/o)	+0.2	0	Sensitized structure <sup>a</sup>
6	Na + UN (41 v/o)	-0.3	0	Sensitized structure <sup>a</sup>
3	Na + UN (40 v/o) + Na <sub>2</sub> O (4000 ppm)	-0.3	0	Characteristic austenitic twinned structure

<sup>a</sup>Carbides precipitated in grain boundaries.

<sup>b</sup>Hyperstoichiometric UC (5.2 w/o C).

In two experiments, 4000 ppm of sodium monoxide was added to the corrosion capsules to evaluate the effect of oxygen contamination. One capsule contained pure sodium, the other a sodium-uranium mononitride paste. With pure sodium the oxygen content resulted in intergranular corrosion of the stainless steel coupon; however, no such corrosive attack occurred for the coupon exposed to a sodium-uranium nitride paste with sodium monoxide present.

\*Hyperstoichiometric with respect to carbon content.

<sup>4</sup>Quarterly Technical Progress Report, NAA-SR-10501, July-Sept 1964.

<sup>5</sup>Quarterly Technical Progress Report, NAA-SR-10850, Oct-Dec 1964.

## G. Plutonium Recycle Reactors

### 1. EBWR Facility

a. Primary Piping. Further repairs of the austenitic stainless steel piping welds were deferred in order to ascertain the causes for the high rejection rates for welds already repaired. Examinations of sectioned, defective welds revealed root defects believed to be associated with thin (less than 1/16-in. thick) weld rootlands. In the heliarc root welding pass, the heat required to melt the Grinnell-type consumable insert overheated the land region, which resulted in an inward shrinkage similar to a "pipe" in castings. A welding procedure utilizing consumable rings, coupled with better welding-groove preparations, is now being utilized with substantial improvements of the root pass weld.

b. Feed Water Filters. The cracked circumferential shell-to-lower head weld of Feed Water Filter No. 1 was repaired. The repaired region has not yet been re-radiographed. The flanged cover-dome connecting-weld was built up by the Central Shops to the required contour to reduce the stresses in the "hub" region of the connection.

c. Reactor Pressure Vessel Cladding. Metallographic examinations and microhardness traverses of three "Boat" samples removed from the EBWR pressure vessel, panels 1, 5, and 8, were partially completed. All panels (No. 1--through-cracks, No. 5--described previously as "sound," and No. 8--which contained very fine superficial surface cracks) contained unsurfaced cracks originating at either the juncture of cladding to SA 212B steel interface or the spot welds. None of the cladding cracks propagated across the interface into the SA 212B pressure vessel steel.

Examinations of the SA 212B pressure vessel steel revealed that the interface surface contained several shallow cracks ranging from 0.001 to 0.010 in depth; they are either grinding cracks generated by the surface grinding of the plate prior to cladding or as rolled plate defects. A number of the deeper surface cracks were found filled with 304 SS intrusions from the spot welding operations. None of these cracks propagated in service. A thin peppery zone of carburized SS 304 was found very close to the interface, and a white decarburized zone in the SA 212B steel. A preliminary microhardness probe across one of the nugget regions showed that the hardness of the cladding was approximately the same as the SA 212B base metal (200 DPH -- 100-gm load) except in the carbon-transfer zones. The slightly carburized SS 304 was 300 DPH, whereas the decarburized SA 212B steel was 150 DPH.

Metallographic data from the 1959 test plate (2-in. SA 212B clad with SS 304) are showing very similar structures at the bonded and unbonded sections of the interface: (1) crack arrest by either the interface

or spot-weld, (2) minor grinding cracks in the SA 212B, (3) minor carburization of SS 304 cladding, (4) shallow decarburization of SA 212B, (5) intrusions of molten SS 304 during cladding, and (6) dirty steels.

The Strauss corrosion-resistance tests showed that all the cladding samples removed from the EBWR pressure vessel and the 1959 test plate were sensitized. The general metallographic condition of all cladding examined showed carbides in the grain boundaries.

These data from both the EBWR Pressure Vessel and the 1959 clad test plate indicate that the cladding failures were probably low-ductility, high-temperature stress ruptures initially. Subsequent stress-rupture failures are believed to have been induced by residual stresses generated in cooling from elevated temperatures during vessel fabrication processes (resistance welding, normalizing heat treatments, and stress-relief cycles).

### III. ADVANCED SYSTEMS RESEARCH AND DEVELOPMENT

#### A. Argonne Advanced Research Reactor (AARR)

##### 1. General

Contract negotiations were completed with Burns and Roe, Inc., of New York for architect-engineer services. An initial three-day meeting between key Burns and Roe and ANL personnel was held at the Laboratory to acquaint the Burns and Roe personnel with the preliminary design concept for the facility and with the supporting research and development program. Subsequently Burns and Roe initiated the planning and indoctrination phase of Title I work, which includes the preparation of PERT/TIME networks and the PERT/COST Work Breakdown Structure for incorporation into the Laboratory's PERT system for AARR.

##### 2. Critical Experiments

The basic program of measurements planned for the 810-fuel-foil system has been completed. Since there is insufficient fuel on hand for loading the 1215-fuel-foil core, additional experiments will be performed with the present loading. One such set of experiments now in progress consists of physics measurements of various types with hollow, square-cross-section aluminum tubes which simulate beam tubes.

Substantial delays in the critical-experiment program have resulted from failure of the fuel-foil supplier to maintain a schedule of deliveries of foils which satisfy the specifications of the contract. A large fraction of the foils delivered to the Laboratory have failed to meet specifications of chemical purity, dimensional requirements, or both. Core-loading changes have been made more difficult because some of the fuel foils are rippled. The number of rippled foils must be limited to ensure that a full core loading can be assembled. More generally, a number of the reactor physics experiments involve measurements of small changes of reactivity or detailed "flux" measurements. The quality of the fuel foils yet to be delivered must be improved so that such measurements may be interpreted meaningfully.

The Laboratory is attempting to accelerate the delivery of fuel foils of higher quality. This has included visits to the fuel-foil supplier, detailed discussions, and careful, on-the-spot inspections. Although there has been no significant change in delivery schedule as yet, the rejection rate has been reduced and foil quality is much improved. Nevertheless, it is not likely that a full core loading will be available until September or October 1965.

Radial and vertical ( $U^{235}$ ) fission traverses have been made with highly enriched U-Al foils in the 810-fuel-foil system. Foil locations,

shown in Figure 15 are similar to those of the 615-fuel-foil system without Plexiglas in the reflector. For given peak activity levels in the Internal Thermal Column and in the beryllium reflector, the activity level in the fuel region is 20% lower in the 810-foil system than in the 615-foil system. This is shown both in the radial traverses and in the vertical traverses (see Figures 16 and 17) respectively.

The temperature coefficient of reactivity was measured in the 810-fuel-foil system. Two cases were studied. In one set of experiments, the reactor was brought to criticality by adjusting water level, with control blades withdrawn. In a second set of experiments, the water level was kept high and control blades were positioned for criticality and calibrated at two different water temperatures, 23°C and 76°C (see Figure 18). The data were corrected for the change in control-blade calibration with temperature; the integral reactivity worth of control blade No. 9 was measured to be higher by 3.3% at 76°C relative to the total worth at 23°C. For each of the two cases, a temperature coefficient of reactivity of  $-0.002\%/^{\circ}\text{C}$  was inferred. This is the same value obtained from critical-water-level experiments with

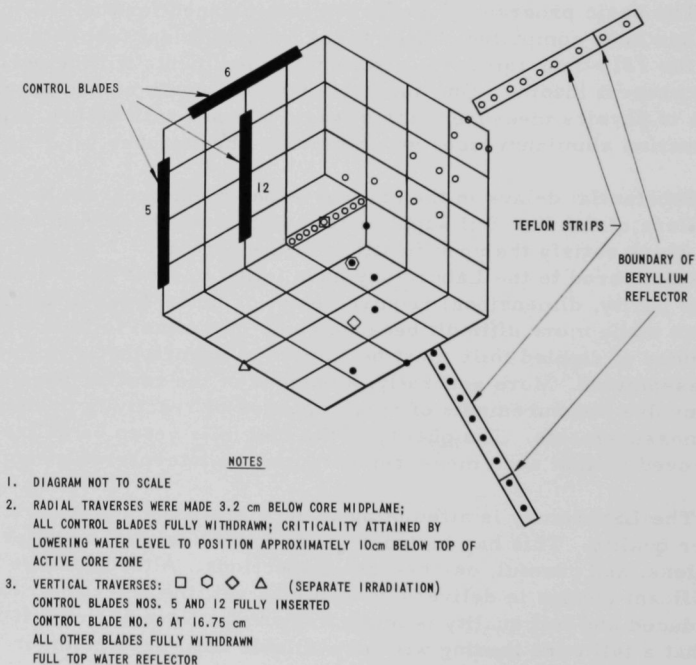


Figure 15. Foil Locations for Radial and Vertical Traverses with Bare U-A1 Foils in the 810-fuel-foil System ( $\text{U}^{235}$  Fission)

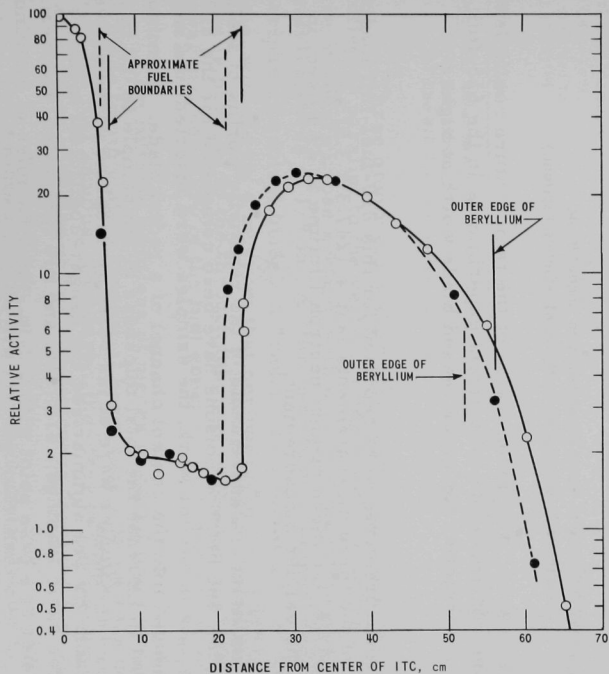


Figure 16. Radial Traverses with Bare U-Al Foils in the 810-fuel-foil System ( $U^{235}$  Fission). (Criticality attained by adjusting level of water in the core.)

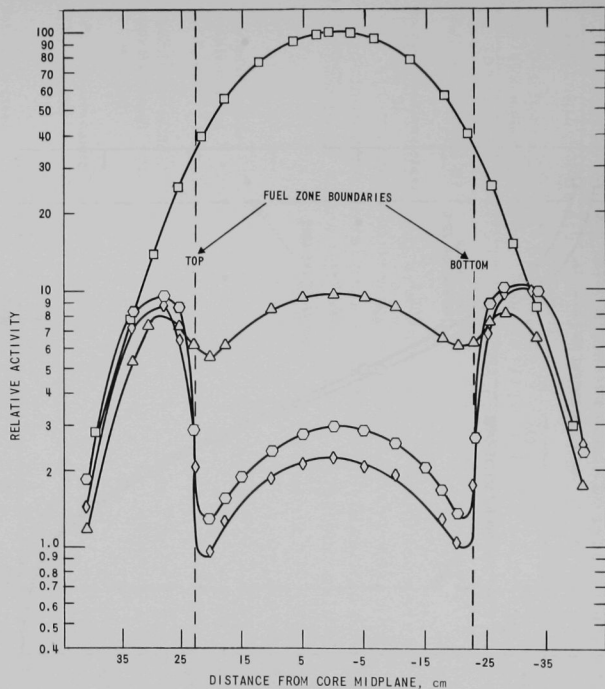


Figure 17. Vertical Traverses with Bare U-Al Foils in the 810-fuel-foil System ( $U^{235}$  Fission). (Criticality attained by insertion of control blades-- see Figure 13.)

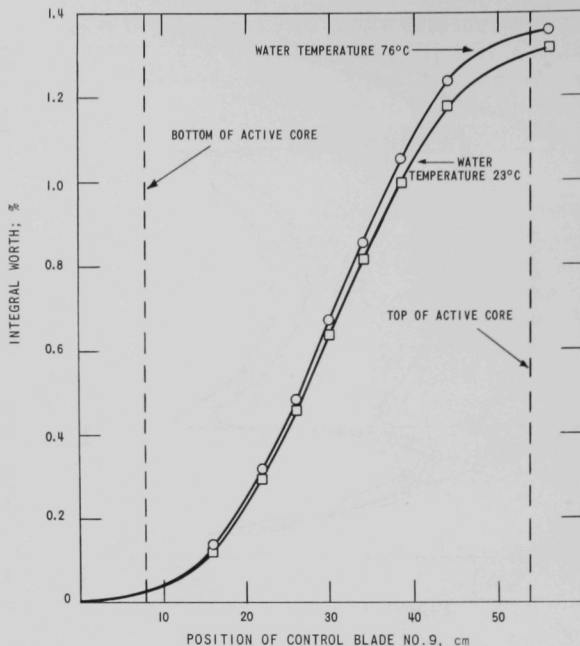


Figure 18. Influence of Water Temperature on Control Blade Calibration. (Control blade No. 9; 810-fuel-foil system.)

the 615-fuel-foil system. A different value of the temperature coefficient was inferred from control-blade-adjustment experiments in the 615-foil loading, without a correction for an increased blade worth at higher temperature.

Rossi- $\alpha$  measurements were repeated for this 810-fuel-foil loading. The mean value of the three measurements is  $\alpha = (247.3 \pm 3.5) \text{ sec}^{-1}$ . Using  $\beta_{\text{eff}} = 0.00726$ , the mean prompt neutron lifetime is  $29.4 \mu\text{sec}$ , in agreement with the earlier measurement.

Danger-coefficient measurements of the reactivity worths of fuel, structural material, and neutron poisons have been completed for the 810-fuel-foil system. As in earlier work, the samples were inserted in a sample holder and introduced into the control channel of a radial blade. Aluminum strips were added to increase the total thickness of the sample to 0.2 in., when necessary. The samples were at the vertical midplane of the active core zone. In Table XV are summarized the danger-coefficient measurements in the three basic loadings: 315, 615, and 810 fuel foils. The reactivity changes refer to a base point with 0.2-in.-thick samples of aluminum.

Table XV. Reactivity Worths of Small Samples in AARR Criticals

Description of Samples	Material Thickness, in.	Reactivity Worth, $10^{-2}\%$		
		315-fuel-foil System	615-fuel-foil System	810-fuel-foil System
Boral (B <sub>4</sub> C-Al; 22.2 w/o B)	0.200	-12.07	-10.15	-8.45
Boron-stainless steel (1.01 w/o B)	0.200	-5.71	-	-3.72
	0.100	-	-2.88	-1.91
	0.050	-	-1.46	-1.15
Cadmium	0.200	-7.53	-5.70	-3.89
	0.100	-6.18	-4.47	-3.15
	0.050	-5.49	-3.56	-2.78
	0.010	-4.21	-2.54	-1.78
Europium oxide-stainless steel (31 w/o Eu)	0.156	-12.18	-10.65	-8.63
Gadolinium oxide-stainless steel (0.7 w/o Gd)	0.200	-3.58	-2.34	-1.54
Hafnium-zirconium (97.5 w/o Hf)	0.200	-	-9.97	-8.00
	0.119	-8.78	-7.89	-6.37
	0.100	-	-7.15	-5.83
Stainless steel	0.200	-0.76	-0.53	-0.46
Uranium-Aluminum (17.44 w/o U; U enriched to 93.17% U <sup>235</sup> )	0.182	+1.46	-	+0.42
	0.078	-	+0.36	+0.23
Water	0.200	+0.76	+0.68	+0.51

Notes: (a) Reference point was 0.2 in. of aluminum.

(b) The 615-fuel-foil system included 420 B-SS strips.

(c) The 810-fuel-foil system included 810 B-SS strips.

Three aluminum-walled tubes have been installed in the beryllium reflector parallel to the vertical midplane of the active core. The tubes are of square cross section, with outside dimensions of 4 in. x 4 in. and a wall thickness of 1/8 in. A "through" tube is immediately adjacent to a peripheral control blade. A "radial" tube forms a "tee" with the through tube, with its tip 4 in. from that peripheral blade. The third ("corner") tube is parallel to the through tube and extends to a vertex of the outer hexagonal boundary of the fuel zone.

By suitable additions of pieces of beryllium, the through tube can be made to simulate a tangential beam tube with its tip at various distances from the fuel annulus. Similarly, the other two tubes may be treated as radial tubes with tips at various distances from the fuel zone.

Preliminary results are that the substitution of the three empty tubes for beryllium caused a reactivity loss of 1.2%. Filling the three

tubes with water caused an additional reactivity loss of approximately 0.2%. Filling only the "corner" tube with water resulted in a negligibly small reactivity gain.

The planned physics experiments with these beam tubes include measurements of reactivity effects, and comparisons of relative neutron flux intensity and gamma flux intensity in radial and tangential tubes.

### 3. Heat Transfer

a. Analytical Studies. A study has been initiated to determine the behavior of the reactor during transients occurring at full-power operation. The scope of the investigation includes conditions at and beyond critical heat flux and/or flow instability. The four principal subdivisions of the study are:

(i) review of relevant existing information on the phenomenon of heat transfer beyond burnout;

(ii) review of available computer programs for their applicability to this study;

(iii) formulation of a model with which to predict the effect of heating beyond critical heat flux and/or flow instability in AARR fuel assemblies. Of particular interest are the questions (a) whether the reduction of reactor power following reactivity-induced transients can limit fuel element temperatures to values below the melting point, and (b) if melting does occur, what fraction of the core is involved. The latter will be useful in predicting the magnitude of pressure pulses which may result from fuel element dispersion;

(iv) outline an experimental program for evaluation of the computational model and predicted behavior.

The subject of pressure pulses in heterogeneous water-cooled reactors has been reviewed. Available data indicate that severe pressure pulses (>3000 psi) can occur with rapid dispersion of molten metal, and moderate pressure pulses can occur during rapid power transients involving no melting. It appears that upper limits for these pulses can be set. It also seems that melting of fuel during slow transients is in need of study.

The STDY-3 Code<sup>6</sup> has been reprogrammed for use on the CDC-3600 computer. Execution time has been improved by this change. A modification of this code is being investigated to ascertain whether or not changes required can be made with relative ease. The changes contemplated

---

<sup>6</sup>Pyle, R. S., STDY-3, A Program for the Thermal Analysis of a Pressurized Water Nuclear Reactor During Steady State Operation, WAPD-TM-213 (June 1960).

include use of a film coefficient based on average film temperature, use of the Zenkevich-Subbotin critical-heat-flux correlation, and interpolation by the code of flow-instability conditions. The reasons for making these changes are to improve the predictability of AARR performance and to facilitate comparison of code results with AARR steady-state heat transfer data.

#### b. Experimental Program

(i) Steady-state Tests. Heat transfer data have been obtained on test section III (see Progress Report for April 1965, ANL-7045, p. 54). Tests were conducted on this section to obtain (a) pressure drop versus flow with constant power, while maintaining all other conditions constant. Failure of the experimental section caused the tests to be terminated. A new test section is being installed, and preliminary measurements of void fraction will be started upon completion of this work.

(ii) Transient Heat Transfer Tests. The trial-and-error investigation of power-supply series-parallel arrangements continued, with further improvement in the rise time. Rise time has been reduced from 60 to 46 msec. This investigation is being conducted in the same facilities which are being used for the steady-state heat transfer tests; therefore, it cannot be continued until a new test section is installed in that loop (see above).

A study of instrumentation in transient systems is under way. Particular attention is being devoted to the testing of pressure transducers for calibration and to obtain minimum response-time data.

#### 4. Hydraulic Tests

A simple hydraulic test was conducted to investigate the effect of localized closure of a fuel-assembly coolant channel on the pressure drop versus flowrate relationship. Localized deflections (or "dimples") are of interest as a possible means of supporting fuel plates to maintain channel spacing.

The test section used was 0.040 x 1.25 x 22.0 in. long, formed from 0.010-in. nickel strips. While under pressure of the water flowing inside of the channel, the section was supported by heavy backup plates. These plates provided means of forcing steel balls against the outside wall until the inside walls touched. Six such deflection points were spaced evenly along the axial centerline of the channel over the center 14 in. of its length.

It was found that each deflection point reduced the flow by about 2.75% and that total flow reduction at constant pressure drop was about 17%. Analysis of the data taken, continues.

## 5. Stress Calculations

A computer program has been developed for the computation of the stresses in the neighborhood of a reinforced circular hole in a flat plate to study the stress-concentration factors for different combinations of plate thickness, outlet-wall thickness, and outlet diameter. The location of the point of maximum stress is on the inside surface of the plate, in the longitudinal direction and at the edge of the hole. This agrees with that found in practically all tests, with both photoelastic models and full-scale steel vessels. The outlet-wall thickness has been tentatively selected, and the stresses are plotted in graphs. The stress-concentration factor at the critical point is about 2.2. This stress condition could be improved by increasing the outlet-wall thickness. At the present time, no attempt at such improvement will be made until information regarding gamma heat around the beam-tube penetration is available. The results also indicate that the region between the through tube HT-1S and beam tube HB-1 is the most critical area.

Several calculations have been made on the thermal stresses in the pressure vessel for the carbon steel AS-212, type B. The results indicate that for the same amount of gamma heat, the thermal stresses are considerably less in the carbon steel than in the stainless steel.

### B. Energy-conversion Systems

#### 1. Thermionic Energy Conversion

An experimental thermionic conversion cell, equipped with a tantalum emitter, was used with various alkali-metal vapors and operated at temperatures between 1800 and 2500°C. Under certain operating conditions, the cell could be made to produce a substantial rf component in addition to the normal dc output.

The frequency, amplitude, and power output of the rf component was recorded as a function of alkali-metal vapor pressure, emitter temperature, and emitter-collector distance.<sup>7</sup>

Analysis of the experimental results showed that the simplified theory for ion oscillations developed by Langmuir<sup>8</sup> does not fully account for all of the observed frequencies, nor does it explain how the plasma oscillations are produced and maintained.

<sup>7</sup>Richards, H. K., DC and High Frequency Voltage and Power Output and Interaction in Cesium, Potassium, and Sodium Thermionic Converters, Symp. on High Temperature Conversion Heat to Electricity, Tucson, Arizona, February 19-21, 1964, TID-7687 (1964), p. 163

<sup>8</sup>Tonks, L. and Langmuir, I., Oscillations in Ionized Gases, Phys. Rev. 33, 195-210 (1929).

Based upon the work of Pierce<sup>9</sup> and Spitzer,<sup>10</sup> expressions have been developed which do account for excitation of the rf component. Thus

$$1 = \frac{\omega_e^2}{(\omega - \beta u_e)^2} + \frac{\omega_i^2}{(\omega - \beta u_i)^2} \quad (1)$$

where

$$\omega_e^2 = 4\pi e^2 n_e / m_e; \quad \omega_i^2 = 4\pi e^2 n_i / m_i,$$

with  $\omega$  equal to angular frequency,  $\beta = 2\pi/\lambda$ , average speed given by  $u$ , variable density by  $n$ , and  $m$  mass; subscript "e" refers to electrons and "i" to ions.

Four solutions of Eq. (1) are possible: two for electron oscillations and two for ion oscillations. Since the electron oscillation frequencies are several hundred times greater than the ion frequencies, the solutions for the ion and electron oscillation frequencies are practically independent of each other. The two solutions for ion oscillations can be found by expanding Eq. (1) and simplifying:

$$\omega = \beta u_i \pm \frac{i\beta u_e \omega_i}{(\omega_e^2 - \beta^2 u_e^2)^{1/2}}, \quad (2a)$$

where

$$\omega_e^2 > \beta^2 u_e^2;$$

$$\omega = \beta u_i \pm \frac{\beta u_e \omega_i}{(\beta^2 u_e^2 - \omega_e^2)^{1/2}}, \quad (2b)$$

where

$$\omega_e^2 < \beta^2 u_e^2.$$

The conditions for exciting ion oscillation are given by Eq. (2a), i.e.,  $\omega_e^2 / \beta^2 u_e^2 > 1$ . The conditions for maintaining oscillation are given by Eq. (2b). These equations agree quite well with the experimental results.

<sup>9</sup>Pierce, J. R., Increasing Space Charge Waves, J. Appl. Phys. 20, 1060-1066 (1949).

<sup>10</sup>Spitzer, L., Physics of Fully Ionized Gases, Interscience Publishers, Inc., New York (1956).

## IV. NUCLEAR SAFETY

### A. Reactor Kinetics

#### 1. Fast Reactor Safety

a. Coolant (Water) Expulsion Studies. Dynamic calibrations of the strain-gauge pressure transducer will be necessary to interpret the experimental results properly. The pressure transducer has been statically calibrated and found to be linear within  $\pm 1/4\%$ .

Several schemes are being investigated in order to obtain a satisfactory determination of the usable frequency response of the transducer; the first is the measurement of a sudden drop in pressure resulting from a punctured diaphragm in a small-volume pressurized vessel, the second uses a shock tube, and the third is the measurement of a sinusoidal pressure variation using an oscillating piston in a cylinder. At least two, and possibly all three, of these techniques will be employed. Information on frequency response is not available from the manufacturer.

Some difficulty has been encountered in the attenuating circuits used in conjunction with the recording oscillograph. These circuits are accordingly being rechecked and modified where necessary.

#### 2. Pressure-pulse Scaling Laws

During the analytical investigation of parametric dependence of pressure and velocity of liquid masses being expelled from heated channels by vaporizing coolant, a series of approximate scaling laws were derived to correlate computer output and to show the relative influences of physical quantities for constant parameters and properties (see Progress Report for May 1965, ANL-7046, pp. 78-79). As derived, the scaling relationships included a quantity  $c$ , defined as the reciprocal of the derivative of pressure with respect to enthalpy. Because, in general, the heated mass of coolant is not identical with the total mass to be accelerated by the pressure,  $c$  must be scaled by the ratio of heated mass to total mass. This implicit dependence on mass must be taken into account in addition to the explicit parametric dependence of the scaling relationships.

In order to clarify the scaling laws, the approximate analytical representation (see Progress Report for December 1963, ANL-6810, pp. 53-54) has been reformulated in terms of specific power  $q$ , defined by

$$q = \text{total power} / \text{heated mass}$$

With this change,  $c$  is independent of mass (although, in general, it depends upon heat transfer and geometry as well as basic thermodynamic properties).

For this new formulation, the effective heated mass used to define  $q$  is taken to be the initial heated mass. As the coolant is expelled from the heated channel, the actual heated mass decreases. However, the fraction of total power entering the coolant also decreases as the coolant is expelled, since the thermal conductivity of the liquid is normally much higher than that of the vapor behind the liquid piston. To the first order, these two effects cancel, although this point must be evaluated explicitly if there are large variations in heater power along the axis of the channel.

Although the resulting scaling relationships are consistent with those derived earlier, the forms are different, and direct application is much clearer. The new equations include

$$\Delta P \doteq K_1 \sqrt[3]{q^2 z m / A}$$

and

$$\dot{z} \doteq K_2 \sqrt[3]{q A z^2 / m},$$

where  $z$  is distance of expulsion,  $\dot{z}$  is the velocity,  $\Delta P$  is pressure rise,  $m$  is total mass to be accelerated, and  $A$  is the cross-sectional area upon which pressure is acting.

## B. TREAT

### 1. Operations

Eight samples of SNAP fuel material were irradiated for Atomics International.

One capsule containing two prototype PBF fuel samples was subjected to 10 irradiations for the Phillips Petroleum Company.

Six metal-water reaction samples of HFIR fuel were irradiated during the month. Two were tested in standard capsules in room-temperature water, two were tested in saturated water at 285°C, and two were tested in room-temperature water in transparent capsules.

### 2. Large TREAT Loop

Final assembly of the main 3-in. piping continues to be delayed because three expansion joints have not been received from the supplier. Installation of pipe heaters on all of the installed piping was completed, and the insulating contractor is insulating the parts of the system that will not interfere with the installation of the remaining expansion joints.

In accordance with design criteria, the large test section of the sodium loop must be demountable. An additional requirement for an EBR-II test subassembly is that the thermocouple egress be placed at the bottom of the test section. For this application, a thermocouple-lead exit assembly, identified as a "below-sodium-surface seal," has been designed and fabricated.

This exit assembly basically consists of a hollow bolt inserted into the end of the pressure tube. Tightness is maintained by means of Type 302 SS "O" rings which are kept under compression by a design unique to sodium technology. The thermocouple leads are then passed through the center of the plug and brazed into place.

The prototype of the exit assembly was installed in a high-temperature, high-pressure sodium pot and subjected to thermal cycling, from room temperature to 500°C, and to internal pressures in excess of 150 psig. There has been no indication of leakage, shifting, or loss of integrity or strength after two weeks of test.

The three electrical connectors that are required to maintain power and instrument circuit continuity through the support flange of the surge suppressor pressure container have been ordered. These units, capable of continuous duty at temperatures up to 1000°F, have stainless steel shells, alumina insulation, and removable pins and sockets (silver alloy-power and transducer connectors, chromel and alumel-thermocouple connector). Pressure gauges and directly connected stainless steel, diaphragm-type gauge protectors filled with silicon oil have also recently been ordered to permit visual observation of the local pressures in the gas system during loop-charging and gas-transfer operations.

The drip pan which is to be located at the top of the reactor has been received.

Difficulty has been encountered in the purchase of Zircaloy for the new liner. A shortage of reactor-grade material from the vendor delays delivery to the extent of 8 to 12 weeks. In addition, a 4-week period is needed for fabrication. However, this item does not affect the construction of the out-of-pile portion of the loop.

Graphite filler fuel elements are being fabricated to fill the void created when reactor core elements are removed to allow room for insertion of the test section.

### 3. Integral Sodium Loops

The integral sodium loops have been instrumented with miniaturized electromagnetic flowmeters and special pressure transducer subassemblies

to measure sodium flowrates in the loops. Flow rates calculated from the outputs of the two types of instruments were not in good agreement.

In order to solve this discrepancy, an apparatus was set up to obtain experimental data relating pressure drop to flow for water. An actual loop test section was used in the flow test to provide an exact geometrical mock-up of the sodium loop components. The experimental curve agreed closely with calculations (see Figure 19), indicating that the pressure data should serve as reference for determining loop flow. Using both measuring systems provides, of course, greater reliability.

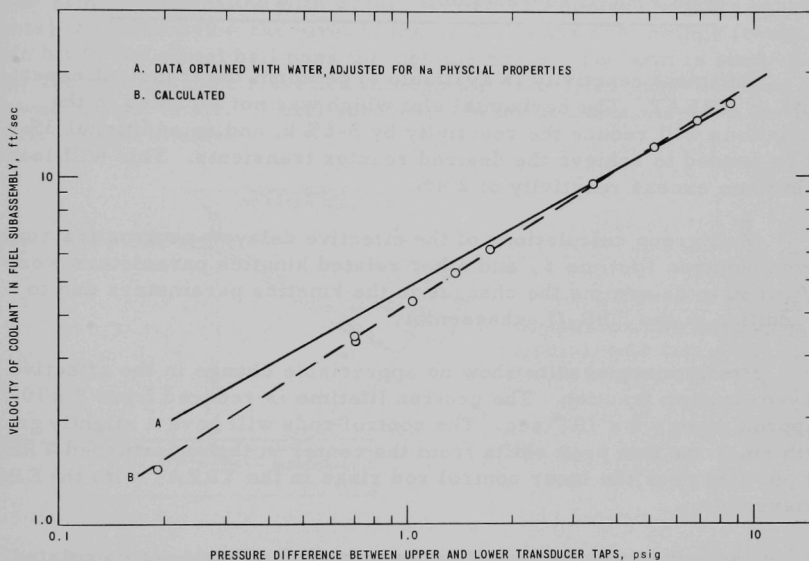


Figure 19. Comparison of Calculated and Experimental Results Obtained for Correlating Pressure Drop and Coolant (Na) Velocity in the Small Loop

#### 4. Physics Analysis of TREAT with an EBR-II Subassembly in Test Hole

Reactivity calculations have been completed using the two-dimensional transport code (DDF-2) and the one-dimensional diffusion code (REX). The results are presented in Table XVI. The differences in the values of "k" are partly explained by the fact that different convergence criteria were required of DDF-2 and REX. Another source of disagreement is the estimated equivalent height used in the REX problems. In view of these differences in input information, the agreement between the DDF-2 and REX results is considered acceptable.

Table XVI. Results of Calculations of  
Reactivity in TREAT

System	Calculated k	
	DDF-2	REX
141-element TREAT	1.002	1.00
Fully loaded TREAT	1.210	1.186
Fully loaded TREAT with EBR-II subassembly	1.140	1.114

Sufficient reactivity is available to perform the transient experiments in TREAT. The horizontal slot which was not included in the calculations will reduce the reactivity by 5-6% k, and an additional 3% k will be needed to achieve the desired reactor transients. This will leave a minimum excess reactivity of 2.4%.

Multigroup calculations of the effective delayed-neutron fraction  $\beta$ , prompt-neutron lifetime  $\ell$ , and other related kinetics parameters were performed to determine the changes in the kinetics parameters due to the addition of the EBR-II subassembly.

Preliminary results show no appreciable change in the effective delayed-neutron fraction. The neutron lifetime is reduced from  $9 \times 10^{-4}$  sec to approximately  $5 \times 10^{-4}$  sec. The control rods will have a slightly greater worth since the flux peak shifts from the center in the unperturbed TREAT to a position near the inner control rod rings in the TREAT with the EBR-II subassembly.

The new temperature coefficient for TREAT was not calculated, for it should be more negative primarily because of increased leakage from the core and reflector. Since the neutron density is peaking closer to reflector when the subassembly is inserted, more neutrons have a greater probability of leaking as the temperature increases. In addition, the test section serves as a sink for neutrons and an increase in the TREAT temperature will allow more neutrons to diffuse into this sink.

### C. Chemical and Associated Energy-transfer Problems in Reactor Safety

#### 1. Studies of Transient Heat Transfer

In order to analyze the consequences of a reactor incident in which hot fuel materials may be dispersed into a liquid coolant, knowledge of the rate and quantity of energy transfer that occurs between the fuel particles

and the coolant is necessary. Neither theoretical nor experimental information is available for the calculation of the heat transfer that occurs when small particles at high temperatures are rapidly dispersed in either water or a liquid metal such as sodium.

An experimental effort to study transient heat transfer from small hot particles moving through a liquid coolant has been initiated. The apparatus (see Figure 20) consists of a swinging arm (or pendulum) with a knife blade attached to the arm. A small metal sphere is attached to a thermocouple at the end of the blade. The metal sphere is heated to the desired temperature in an electrically heated tube furnace prior to release of the arm. A tank filled with water (sodium will be used in later experiments) is placed below the pivot of the arm. As the arm swings freely, the knife blade and metal ball pass through the water. The arm is stopped after the ball has once travelled through the water; the sphere is then allowed to cool in air. Nickel spheres,  $1/4$  in. in diameter, were used in the first experiments.

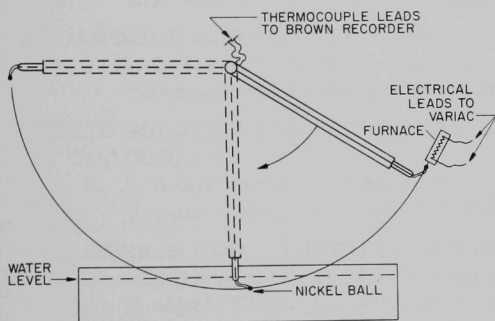


Figure 20

Diagram of Pendulum (Swinging Arm) Apparatus Used in Study of Heat Transfer from Moving Spheres to Water

Two methods were used to attach the nickel spheres to the Pt/Pt, 10% Rh thermocouples. In one, a thermocouple junction was imbedded in a ceramic cement contained in a hole that was drilled through the center of the sphere. In the other, the thermocouple was welded to the surface of the ball, each of the thermocouple leads being welded to the opposite side of the ball, so that the ball was suspended between the two lead wires.

A record is made of millivolt output of the thermocouple on a Brown pen recorder. The relatively slow cooling in air as compared with the very rapid cooling in the water allows determination of the temperature of the ball as it enters and leaves the water. Average heat fluxes can be calculated from the measured temperature drop.

The water was maintained at room temperature, and no attempt was made to deaerate the water. High-speed motion pictures were taken of the ball moving through the water. The time of immersion of the knife blade

was measured electronically. The angular velocity calculated from these measurements was used to obtain the linear ball velocity; the average linear velocity was determined to be about 10 ft/sec.

The distance of travel through the water can be varied by changing the depth of water in the tank. Path lengths of from 21.3 to 30.6 in. have been employed.

Heat fluxes of from 80 to 180 cal/(sec)(cm<sup>2</sup>) have been measured in these preliminary experiments. These are similar to subcooled boiling heat transfer fluxes reported in the literature.<sup>11</sup>

---

<sup>11</sup>P. A. Lottes et al., Boiling Water Reactor Technology: Status of the Art Report, ANL-6561, Vol. I, Heat Transfer and Hydraulics, p. 9.

## V. PUBLICATIONS

Papers

REPROCESSING OF NUCLEAR REACTOR FUELS BY PROCESSES  
BASED ON VOLATILIZATION, FRACTIONAL DISTILLATION, AND  
SELECTIVE ADSORPTION

A. A. Jonke

Atom. Energy Rev. 3(1), 3-60 (1965)

SIMPLIFIED TECHNIQUE FOR USING THE DIAPHRAGM-TYPE LIQUID  
DIFFUSION CELL

J. T. Holmes

Rev. Sci. Instr. 36, 831-832 (June 1965)

MASS TRANSPORT FROM URANIUM SPHERE TO LIQUID CADMIUM  
IN HIGHLY TURBULENT FLOW

E. D. Traylor, Leslie Burris, and C. J. Geankoplis

Ind. Eng. Chem. Fundamentals 4(2), 119-125 (May 1965)

CORROSION EXPERIENCE WITH ALUMINUM POWDER PRODUCTS

J. E. Draley, W. E. Ruther, and S. Greenberg

International Journal of Powder Metallurgy 1(2), 28-41 (1965)

SOLID SOLUTIONS IN THE SYSTEM URANIA-RARE EARTH OXIDES.  
I.  $UO_2-GdO_{1.5}$

R. J. Beals and J. H. Handwerk

J. Am. Ceram. Soc. 48, 271-274 (May 1965)

AN OPERATIONAL THERMAL NEUTRON IMAGE INTENSIFIER

Harold Berger, W. F. Niklas, and Adolph Schmidt

J. Appl. Phys. 36, 2093-2094 (June 1965)

COMMENTS ON "ON CLOSED LOOP OPTIMAL CONTROL"

Isaac Kliger

IEEE Trans. AC-10(2), 207 (April 1965) Letter

LAMINAR FILM CONDENSATION IN THE PRESENCE OF AN ELECTRO-  
MAGNETIC FIELD

R. M. Singer

Mech. Eng. 87, 63 (June 1965)

RADIATION BETWEEN CONCENTRIC CYLINDERS WITH  
PERFORATIONS

R. P. Stein

J. Heat Transfer 87, 316 (May 1965) Note

CALCULATION OF SPECTRAL DISTORTION DUE TO PILE-UP EFFECT  
Raymond Gold

Rev. Sci. Instr. 36, 784-794 (June 1965)

## DESEGREGATING THE ATOM

B. I. Spinrad

Nucl. News 8, 3 (June 1965)

## ELASTIC NEUTRON SCATTERING FROM INTERMEDIATE-WEIGHT ELEMENTS

S. A. Cox

Bull. Am. Phys. Soc. 10, 576 (June 1965) Abstract

## FAST-NEUTRON CROSS SECTIONS OF Na AND Al

Ji-Peng Chien and A. B. Smith

Bull. Am. Phys. Soc. 10, 576 (June 1965) Abstract

The following appeared as abstracts in the Transactions of the American Nuclear Society 8(1), (June 1965):

## DETERMINATION OF BURNUP ON EBR-II FUEL

R. P. Larsen

p. 8

STRUCTURE OF U<sup>20</sup> wt% Pu-Fs ALLOYS

O. L. Kruger

p. 28

## ON THE THERMAL STRESS ENDURANCE OF NUCLEAR FUELS

A. J. Carrea and J. F. Schumar

pp. 45-46

## A THERMAL-NEUTRON TELEVISION SYSTEM FOR POSTIRRADIATION ANNEALING STUDIES

Harold Berger and W. N. Beck

pp. 73-74

## STABILITY MEASUREMENTS ON THE BORAX-V PERIPHERAL SUPERHEATER CORE

D. C. Cutforth and Dale Mohr

p. 106

## REACTOR DEACTIVATION, EBR-I AND BORAX-V

J. D. Cerchione, F. D. McGinnis, R. E. Rice, and C. B. Doe

pp. 114-115

## METAL-WATER REACTIONS INITIATED BY A SHORT-PERIOD NUCLEAR REACTOR EXCURSION (KIWI-TNT)

R. C. Liimatainen, R. O. Ivins, and F. J. Testa

pp. 131-132

## ENGINEERING DEVELOPMENT OF A PRACTICAL 1200° SODIUM-VAPOR TRAP

E. L. Kimont

p. 147

## FARET FUEL ASSEMBLY FLOW TEST LOOP

R. H. Armstrong and F. A. Smith

pp. 149-150

## FUEL PROPERTIES AND NUCLEAR PERFORMANCE OF FAST REACTORS FUELED WITH MOLTEN CHLORIDES

P. A. Nelson, D. K. Butler, M. G. Chasanov, and David Meneghetti

pp. 153-154

## STUDY OF REFLECTOR-BASED CONTROL OF FAST NUCLEAR ROCKET REACTORS

K. K. Almenas

pp. 165-166

## SPATIAL DEPENDENCE OF THE DECAY RATES OF PROMPT-NEUTRON CHAINS IN REFLECTED REACTORS

R. A. Karam

pp. 224-225

## OPTIMAL CONTROL OF A SPACE-DEPENDENT NUCLEAR REACTOR

Isaac Kliger

pp. 233-234

## USE OF BERYLLIUM ZONES TO ENHANCE SAFETY OF FAST BREEDER REACTORS

D. K. Butler, H. H. Hummel, W. B. Loewenstein, and David Meneghetti

pp. 239-240

## PHYSICS MEASUREMENTS OF MODIFIED TUNGSTEN-BASED ALUMINUM-REFLECTED FAST REACTORS

W. G. Knapp, R. C. Doerner, K. K. Almenas, C. E. Cohn, and

R. A. Karam

p. 241

## EFFECTIVE FISSION-RATIO MEASUREMENTS IN A SERIES OF FAST REACTORS

G. W. Main, F. H. Helm, and H. H. Meister

pp. 242-243

## CRITICAL FACILITY MEASUREMENTS OF THE SODIUM-VOID COEFFICIENT IN A LARGE DISC-SHAPED FAST-REACTOR CORE

F. H. Helm, W. Y. Kato, G. W. Main, H. H. Meister, and G. K. Rusch

pp. 245-246

## THE INFLUENCE OF HETEROGENEITY ON THE MEASURED SODIUM-VOID COEFFICIENT IN A 950-LITER PANCAKE FAST CORE

G. K. Rusch and F. H. Helm

pp. 246-247

## EVALUATION OF GROUP SECTIONS FOR LIGHT REFLECTORS OF FAST REACTORS

David Meneghetti

pp. 247-248

EXPERIMENTAL THERMAL-DISADVANTAGE FACTORS IN SOME VERY UNDERMODERATED 3%-ENRICHED, WATER-URANIUM OXIDE LATTICES

A. R. Boynton  
p. 249

PRECISION REACTIVITY MEASUREMENT FACILITY AT ARGONNE NATIONAL LABORATORY

R. C. Doerner  
pp. 261-262

LINEAR RELATIONSHIP BETWEEN CADMIUM RATIO AND REACTOR CORE COMPOSITION

G. S. Stanford and K. E. Plumlee  
pp. 270-271

A METHOD OF CALCULATING MUTUAL SHIELDING BETWEEN RESONANCES OF DIFFERENT NUCLIDES

P. H. Kier  
pp. 286-287

RESONANCE INTEGRALS IN SLAB LATTICES USING VARIOUS ESCAPE PROBABILITIES

E. M. Pennington  
pp. 288-289

REACTION OF URANIUM WITH WATER IN TREAT MELTDOWN EXCURSION

R. C. Liimatainen, R. O. Ivins, and F. J. Testa  
p. 306

METAL-STEAM REACTIONS AT HIGH TEMPERATURES

R. E. Wilson and Charles Barnes  
pp. 306-307

FAST-REACTOR SAFETY EXPERIMENTS ON EBR-II-TYPE THORIUM-URANIUM FUEL

C. E. Dickerman, L. E. Robinson, and R. R. Stewart  
p. 309

ANL Reports

ANL-6928 CONSOLIDATION AND FABRICATION TECHNIQUES FOR VANADIUM-20 w/o TITANIUM (TV-20)

W. R. Burt, Jr., W. C. Kramer, R. D. McGowan,  
F. J. Karasek, and R. M. Mayfield

ANL-6961 EXPERIMENTS WITH CENTRAL SUPERHEATER CORE CSH-1, BORAX-V

BORAX-V Project Staff

ANL-7020 CHEMICAL ENGINEERING DIVISION RESEARCH HIGHLIGHTS, May 1964--April 1965



3 4444 00007681 0